BELLE-NOTE-XX-YYYY-ZZZ
DRAFT Version 0.0
July 29, 2022

Measurement of inclusive $B \to \Lambda_c$ branching fractions using Belle data and hadronic Full Event Interpretation

Leonardo Benjamin Rizzuto

Institute Jožef Stefan, Ljubljana, Slovenia

Abstract

Inclusive $B \to \Lambda_c$ branching fractions were measured most recently by BaBar collaboration. However, the measurement still presented a poor accuracy. A more precise measurement of inclusive $B \to \Lambda_c$ branching fraction could be useful to gain a better confidence on B meson weak decays treatment.

Contents

1. INTRODUCTION

Inclusive B meson baryonic decays with a Λ_c baryon in the final state are the most abundant, due to a relatively large V_{cb} element of the CKM matrix. The *BaBar* experiment measured their branching fractions to be around the percent level (see ref. [1]). However, the branching fractions were determined with big uncertainties: nearly 50% on the measured values or, in the case of the $B^0 \to \Lambda_c^+$ decay, only an upper limit could be established. A more precise measurement of inclusive $B \to \Lambda_c$ branching fractions may shed light on the appropriateness of B meson weak decays treatment, particularly of strong interaction effects modelling. Predictions for inclusive branching fractions are given, for example, in ref. [2].

Exploiting the Full Evenet Interpretation (FEI) algorithm, developed for the Belle II experiment, it may be possible to perform a more precise measurement of inclusive $B \to \Lambda_c$ branching fractions, performed using the full Belle data set.

2. ANALYSIS SETUP

The reconstruction is performed with `BASF2` release `05-02-03` together with the `b2bii` package in order to convert the *Belle* `MDST` files (`BASF` data format) to *Belle II* `MDST` files (`BASF2` data format). The FEI version used is `FEI_B2BII_light-2012-minos`.

3. DATASETS USED

The Belle detector acquired a dataset of about $L_0 \approx 710 fb^{-1}$ of integrated luminosity in its lifetime at the $\Upsilon(4S)$ energy of 10.58 GeV, which corresponds to about 771 $\times 10^6 B\bar{B}$ meson pairs. Additionally, several streams of Monte-Carlo (MC) samples were produced, where each stream of MC corresponds to the same amount of data that was taken with the detector. No specific signal MC was used: instead of producing dedicated signal MC samples, the samples were obtained by filtering the decays of interest from the generic on-resonance MC samples. The following samples were used in this analysis:

- data
- MC - 10 streams of B^+B^- and $B^0\bar{B}^0$ (denoted as `charged` and `mixed`) for signal decays and backgrounds.
  - 6 streams of $q\bar{q}$ produced at $\Upsilon(4S)$ resonance energy
  - 6 streams of $q\bar{q}$ produced at 60 MeV below $\Upsilon(4S)$ resonance energy, where each stream corresponds to $1/10 \times L_0$.

4. EVENT SELECTION AND RECONSTRUCTION

In this chapter the procedure for reconstruction of the events where one B meson decays inclusively to a Λ_c baryon and the accompanying B meson decays hadronically.

4.1. B_{tag} reconstruction

The FEI is an exclusive tagging algorithm that uses machine learning to reconstruct B meson decay chains and calculates the probability that these decay chains correctly describe the true process. In this analysis only hadronically reconstructed decay chains are considered. The training called `FEI_B2BII_light-2012-minos` is used. Tag-side B meson candidates are required to have a beam-constrained mass greater than 5.22 GeV/c^2 and $-0.15 < \Delta E < 0.07$ GeV.
In the case of multiple candidates in the same event, the candidate with the highest SignalProbability (the signal probability calculated by FEI using FastBDT) is chosen. To suppress the background constisting of B^0 events misreconstructed as B^+ (and vice-versa) from neutral (charged) decays also a B^0 (B^+) candidate is reconstructed with FEI and if the SignalProbability of it is higher than the charged (neutral) reconstructed B meson, the event is discarded. This constitutes a sort of crossfeed-veto, rejecting part of events belonging to the other typology of decays of interest: for example in the case one is interested in reconstructing $B^{+/-}$ decays and the event actually contains $B^0/\bar{B}^0$ decays, the FEI reconstructed neutral B meson candidate most likely presents a higher SignalProbability than the charged FEI reconstructed candidate.

4.2. Λ_c reconstruction

In the *rest of event* (ROE) of the reconstructed B_{tag} meson, to select $\Lambda_c \to pK\pi$ signal candidates, the following event selection criteria are applied. Charged tracks the impact parameters perpendicular to and along the nominal interaction point (IP) are required to be less than 2 cm and 4 cm respectively ($dr < 2$ cm and $|dz| < 4$ cm).
The pion tracks are required to be identified with $\frac{\mathcal{L}_\pi}{\mathcal{L}_K+\mathcal{L}_\pi} > 0.6$. The kaon tracks are required to be identified with $\frac{\mathcal{L}_K}{\mathcal{L}_K+\mathcal{L}_\pi} > 0.6$, and the proton/anti-proton tracks are required to be identified with $\frac{\mathcal{L}_{p/\bar{p}}}{\mathcal{L}_K+\mathcal{L}_{p/\bar{p}}} > 0.6$ and $\frac{\mathcal{L}_{p/\bar{p}}}{\mathcal{L}_\pi+\mathcal{L}_{p/\bar{p}}} > 0.6$, where the $\mathcal{L}_{\pi,K,p/\bar{p}}$ are the likelihoods for pion, kaon, proton/anti-proton, respectively, determined using the ratio of the energy deposit in the ECL to the momentum measured in the SVD and CDC, the shower shape in the ECL, the matching between the position of charged track trajectory and the cluster position in the ECL, the hit information from the ACC and the dE/dx information in the CDC.
For the Λ_c candidates a vertex fit is performed with `TreeFitter`, requiring it to converge. If there are more than one Λ_c combination, then the best candidate based on the χ^2 probability is chosen. The Λ_c signal region is defined to be $|M_{\Lambda_c} - m_{\Lambda_c}| < 20$ MeV/c^2 ($\sim 3\sigma$), here m_{Λ_c} is the nominal mass of m_{Λ_c}.

4.3. Wrongly reconstructed B_{tag} candidates

In the case of the signal sample the distributions for the beam-constrained mass M_{bc} and for the correctly reconstructed Λ_c candidates, look like in Fig. 1. If one then investigates the M_{bc} distribution of the B_{tag} candidates reconstructed with FEI, it can be seen that there is a peaking structure for wrongly reconstructed B mesons (as in Fig. 2), according to the

BASF2 internal truth matching variable **isSignal**. It is obvious from this that the BASF2 internal truth matching variable cannot be used to separate properly the signal events in correctly and wrongly reconstructed B mesons. In the study BELLE2-NOTE-TE-2021-026 `https://docs.belle2.org/record/2711/files/BELLE2-NOTE-TE-2021-026.pdf` a possible solution was found developing new variables that can be used for an improved truth matching for the FEI (those variables were added to a newer BASF2 release than the one used for this study). In the present study instead a more "traditional" approach was adopted: fitting the M_{bc} distribution with a sum of PDFs that account for the flat (background) component and the peaking (signal) component. To validate this method a control decay study was performed on the flavor correlated $B^+ \to \bar{D}^0$ channel.

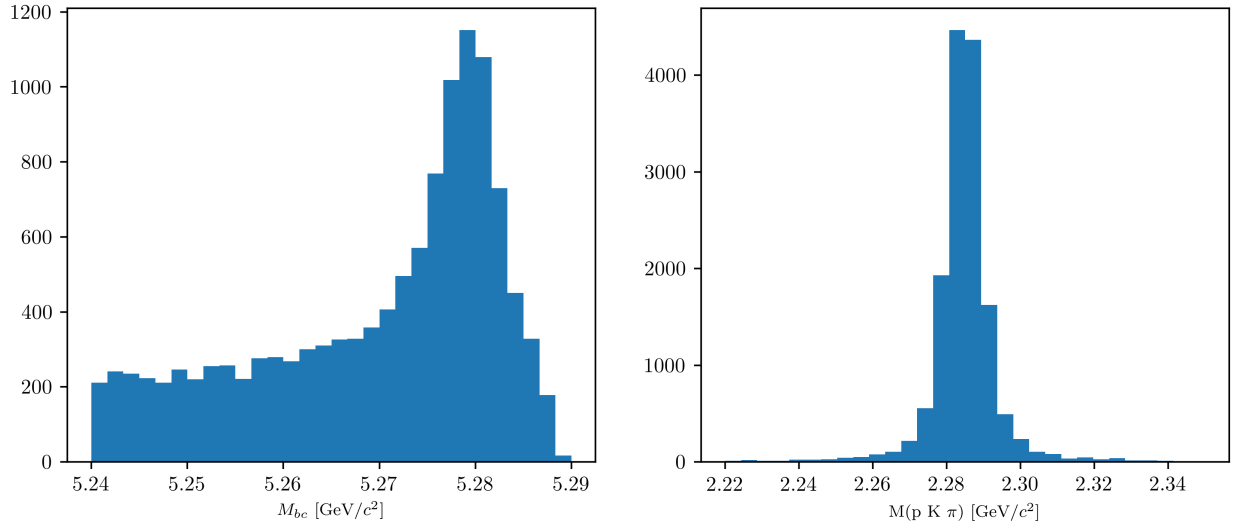

FIG. (1) M_{bc} and $M(pK\pi)$ distributions of B_{tag} and Λ_c candidates reconstructed in the signal sample.

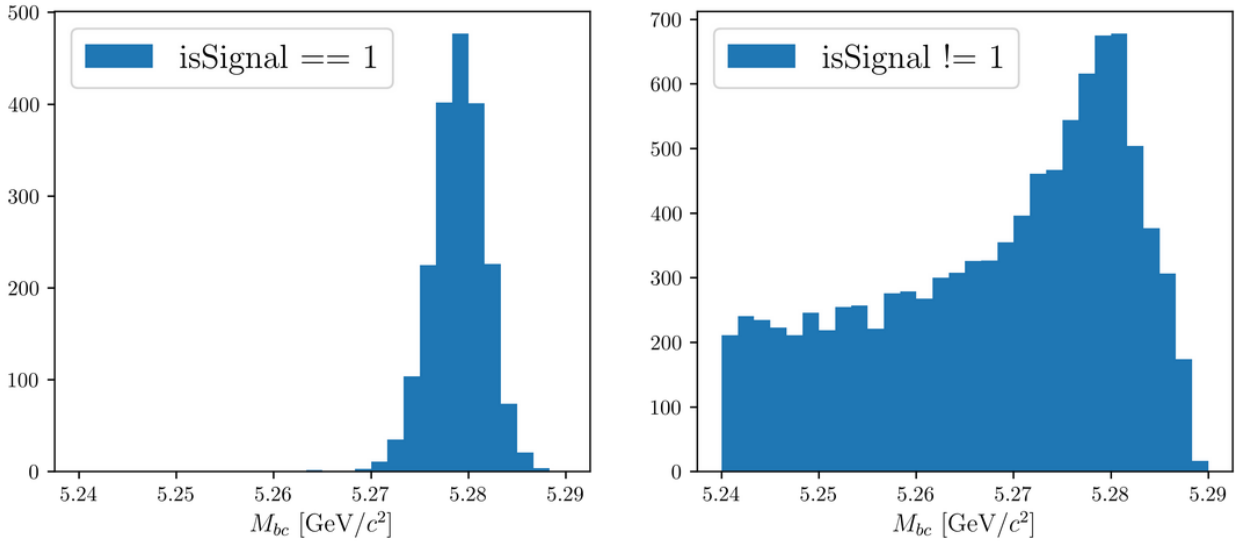

FIG. (2) M_{bc} distribution of B_{tag} candidates reconstructed in the signal sample, truth-matched (on the left) and not (on the right).

5. SIGNAL SELECTION OPTIMIZATION

To further enhance the purity of the signal decays, an optimization procedure is adopted to determine optimal cuts for a set of variables for each decay mode under investigation by this study. The cuts on the following variables are optimized:

- $foxWolframR2$: the event based ratio of the 2-nd to the 0-th order Fox-Wolfram moments
- SignalProbability: the already mentioned signal probability calculated by FEI using FastBDT
- $p^{\Lambda_c}_{CMS}$: momentum of the Λ_c candidates in the center of mass system

The optimization is based on the Figure Of Merit (FOM): FOM $= \frac{S}{\sqrt{S+B}}$
Where S and B are respectively signal and background events in the signal region: $M_{bc} > 5.27$ GeV/c^2, $2.2665 < M(pK\pi) < 2.3065$ GeV/c^2.
Due to the issue reported in Sec. 4 4.3, to separate signal events that peak in M_{bc} from the ones that are not (which are then categorized as background events), the events reconstructed in the signal sample are fitted. with a sum of Crystal Ball function and Argus for each cut value on the corresponding variable to optimize (as in Fig. 3).

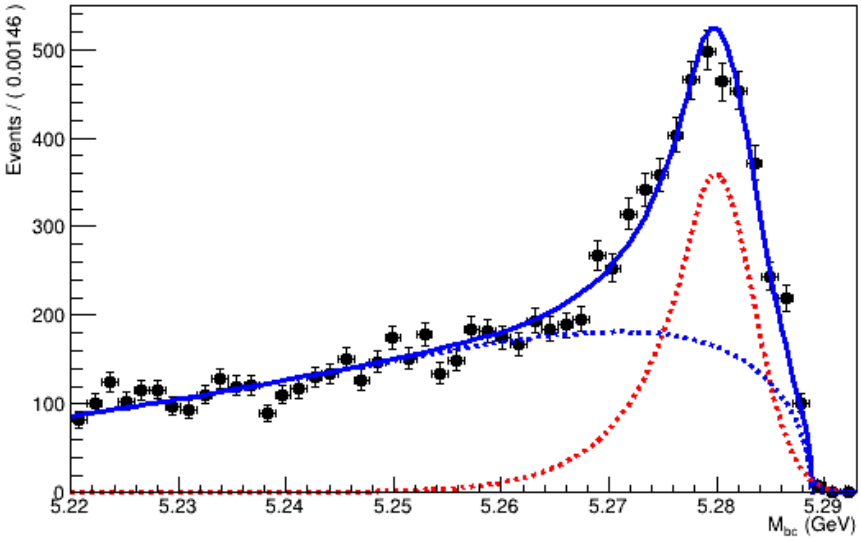

FIG. (3) Example of a fit used to separate the correctly reconstructed B mesons (described by the red dotted Crystal Ball function) from the wrongly reconstructed ones (described by the blue dotted Argus function).

5.1. $B^- \to \Lambda_c^+$ decays

First, in order to suppress the continuum background the cut on $foxWolframR2$ is optimized. Fig. 4 shows the $foxWolframR2$ distributions for signal and continuum events.

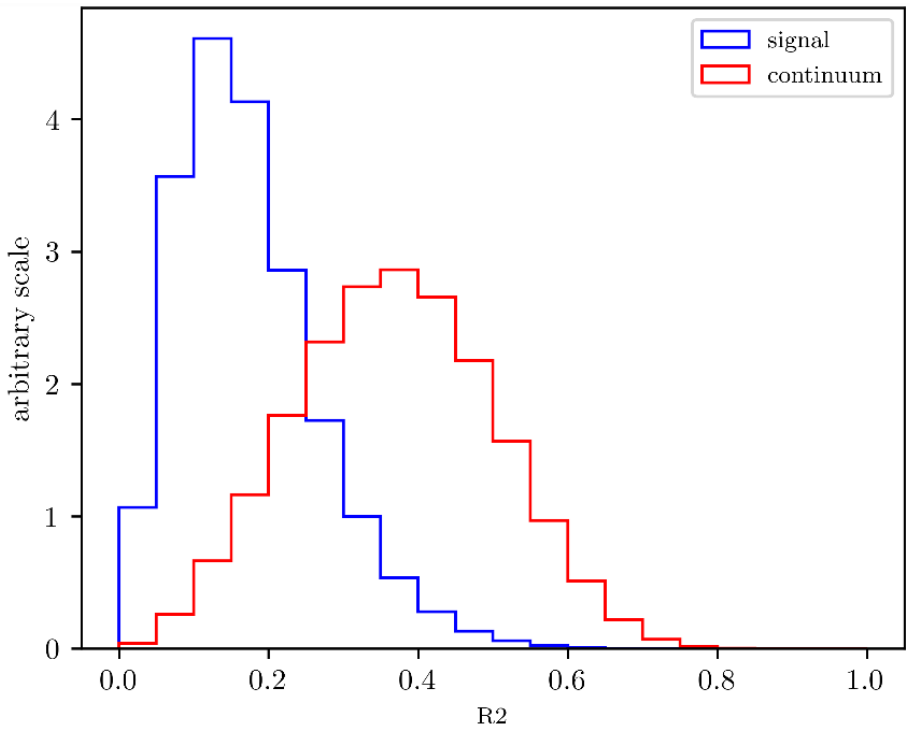

FIG. (4) Distribution of the $foxWolframR2$ variable for signal and continuum background events.

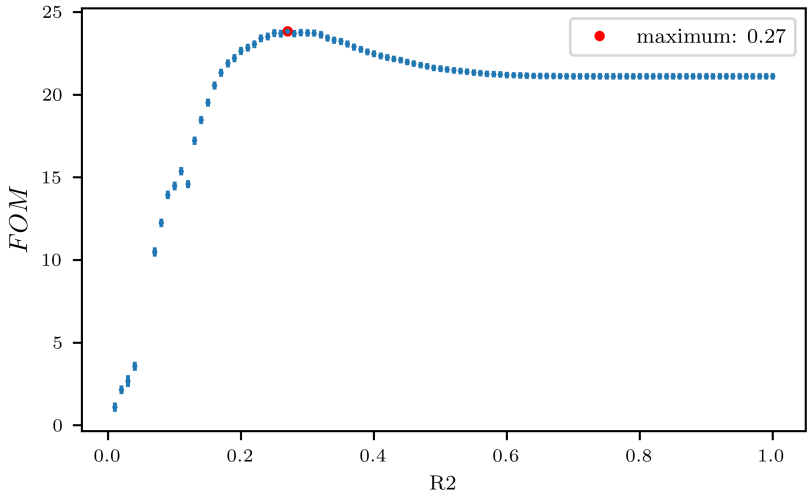

FIG. (5) Figure of Merit values calculated at several cuts on the $foxWolframR2$ variable

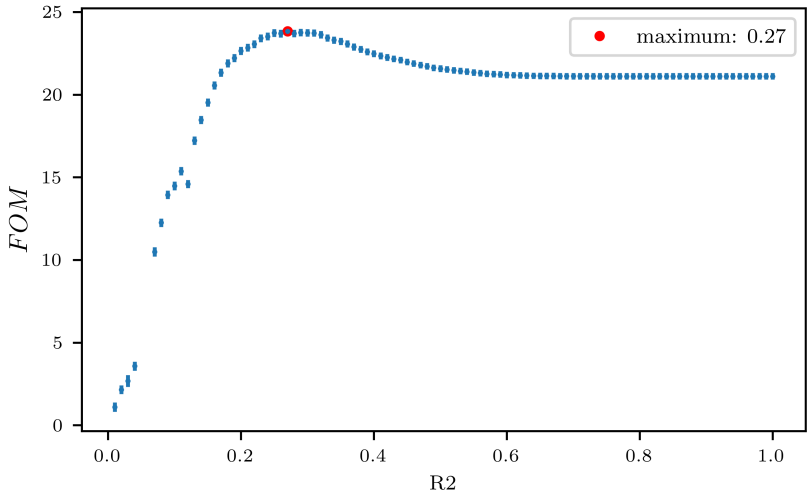

FIG. (6) Figure of Merit values calculated at several cuts on the $foxWolframR2$ variable

With the optimized cut $foxWolframR2 < 0.27$, the cut on SignalProbability is optimized in the same way (see Fig. 7).

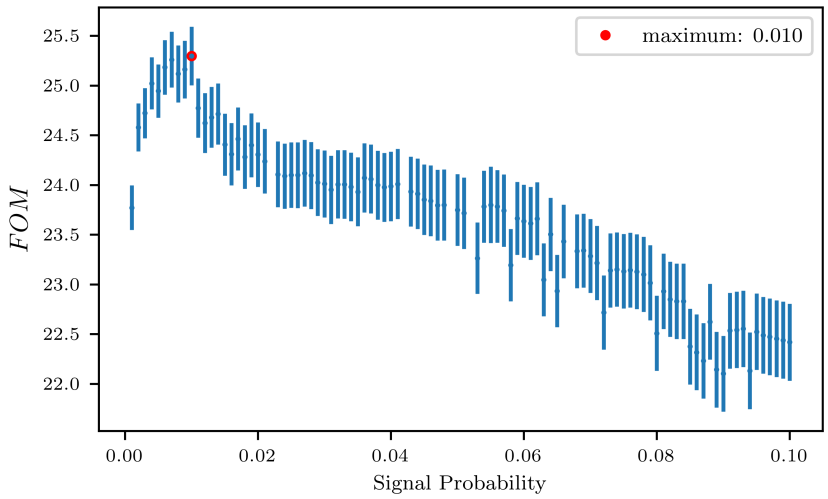

FIG. (7) Figure of Merit values calculated at several cuts on the SignalProbability variable

With the optimized cut SignalProbability > 0.01, the cut on $foxWolframR2$ variable is rechecked (Fig. 8). Being the maximum values fluctuating around $foxWolframR2 < 0.3$, this cut is the one finally chosen for this variable.

With the optimized cuts on SignalProbability and $foxWolframR2$ variable, the cut on $p^{\Lambda_c}_{CMS}$ is optimized

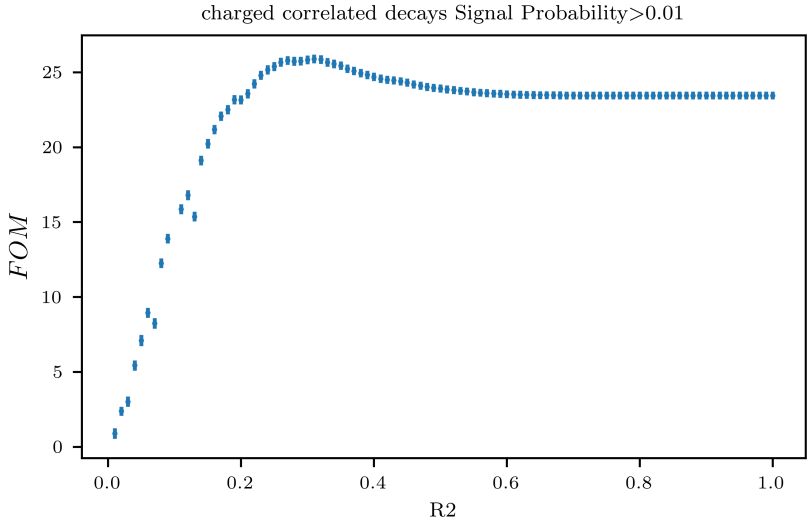

FIG. (8) Figure of Merit values calculated at several cuts on the $foxWolframR2$ variable

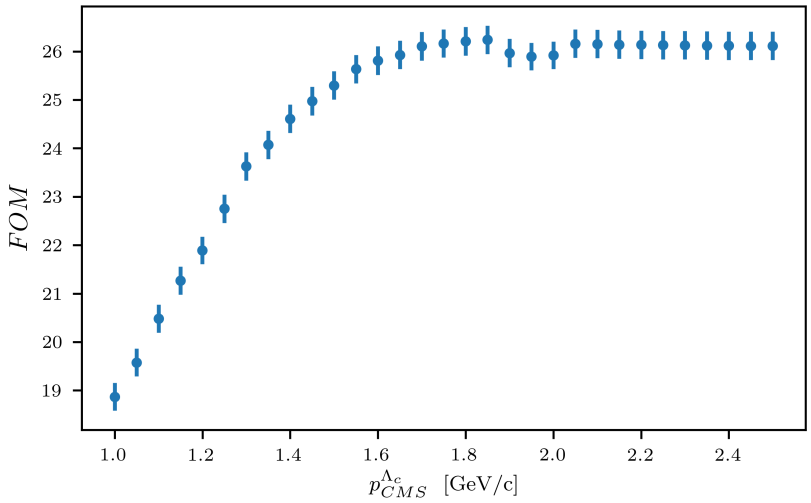

FIG. (9) Figure of Merit values calculated at several cuts on the momentum of the Λ_c candidates in the center of mass system

From Fig. 9 one can see that with values of the cut above $p^{\Lambda_c}_{CMS} < 1.8$ GeV/c^2 a plateau of maximum FOM values is reached. But such a cut would still be useful to reject some background events as one can see from Fig. 10.

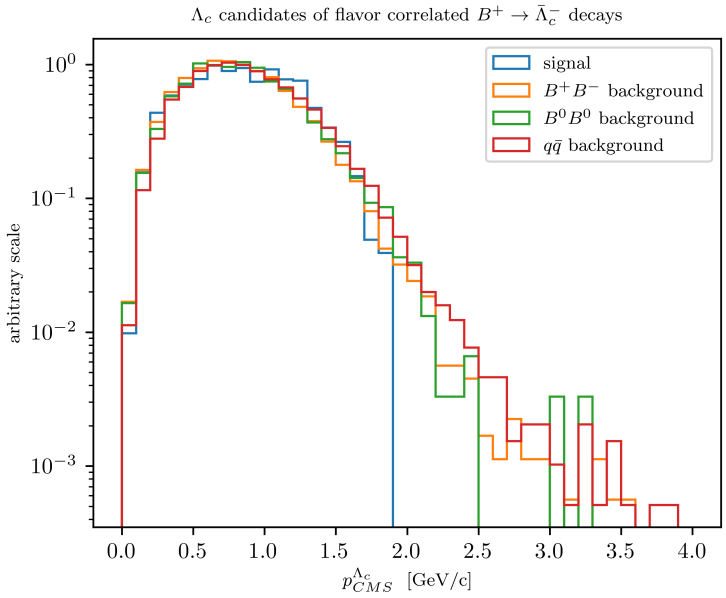

FIG. (10) Distribution of Λ_c candidates momenta in the center of mass system

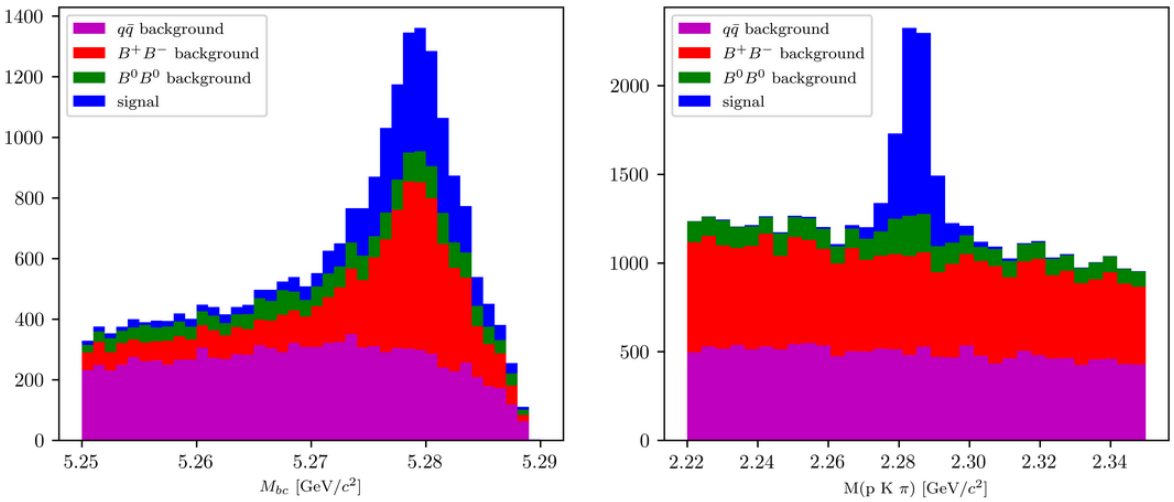

FIG. (11) Distribution of M_{bc} (left) and invariant mass of charged correlated Λ_c candidates (right), in the signal region after the above mentioned selection cuts.

6. FITTING ($B^- \to \Lambda_c^+ X$ DECAYS)

To measure the inclusive branching fraction of $B^- \to \Lambda_c^+ X$ the following quantities need to be known:

$$Br(B^- \to \Lambda_c^+ X) = \frac{N_{tag,\Lambda_c} \cdot \epsilon^+_{FEI}}{N_{tag} \cdot Br(\Lambda_c^+ \to pK^-\pi^+)\epsilon_{\Lambda_c}\epsilon^+_{FEI,sig}} \quad (1)$$

Where

- N_{tag,Λ_c} is the reconstructed signal yield obtained from a two dimensional fit of M_{bc} and $M(pK\pi)$ in the final sample.
- N_{tag} is the reconstructed signal yield obtained from the M_{bc} fit of all the tagged B mesons in the final sample.
- ϵ_{Λ_c} is the Λ_c reconstruction efficiency.
- ϵ^+_{FEI} represents the hadronic tag-side efficiency for generic B^+B^- events.
- $\epsilon^+_{FEI,sig}$ represents the hadronic tag-side efficiency for B^+B^- events where the tagged B meson decays hadronically and the accompanying meson decays inclusively into the studied signal channel.
- $Br(\Lambda_c^+ \to pK^-\pi^+)$: the branching fraction of the decay mode used to reconstruct the Λ_c baryon.

In order to extract N_{tag,Λ_c} and N_{tag} unbinned extended maximum-likelihood fits are performed. The Fit final samples contain both signal and background candidates from various sources. First the fit model that accurately describes the distributions in the $B_{tag} + \Lambda_c$ final sample will be described.

6.1. Probability Density Functions (PDFs) for the two dimensional fit

The PDFs used to describe the signal distributions are discussed first. The final sample of total signal events presents a peak around the expected B meson mass and a tail at low M_{bc} values. The peaking component represents the correctly reconstructed signal events in M_{bc} and therefore denoted from now on as **reconstructed signal**. The flat component on the left side from the peak represents the combinatorial background, i.e. B mesons that were misreconstructed, and therefore those events are denoted from now on as **misreconstructed signal**. The 2D fit shown in Fig. 12 is performed with a sum of the following probability density functions:

- $$P^{recSig}_{B,\Lambda_c}(M_{bc}, M(pK\pi)) = \Gamma_{CB}(M_{bc}) \times \rho_G(M(pK\pi)) \quad (2)$$
- $$P^{misSig}_{B,\Lambda_c}(M_{bc}, M(pK\pi)) = \Gamma_{ARG}(M_{bc}) \times \rho_G(M(pK\pi)) \quad (3)$$

The first is used to fit the reconstructed signal and $\Gamma_{CB}(M_{bc})$ is a Crystal Ball function. The second is used to model the misreconstructed signal and $\Gamma_{ARG}(M_{bc})$ is an Argus function. In both cases a sum of three Gaussian functions $\rho_G(M(pK\pi))$ describes the mass of the Λ_c baryon.

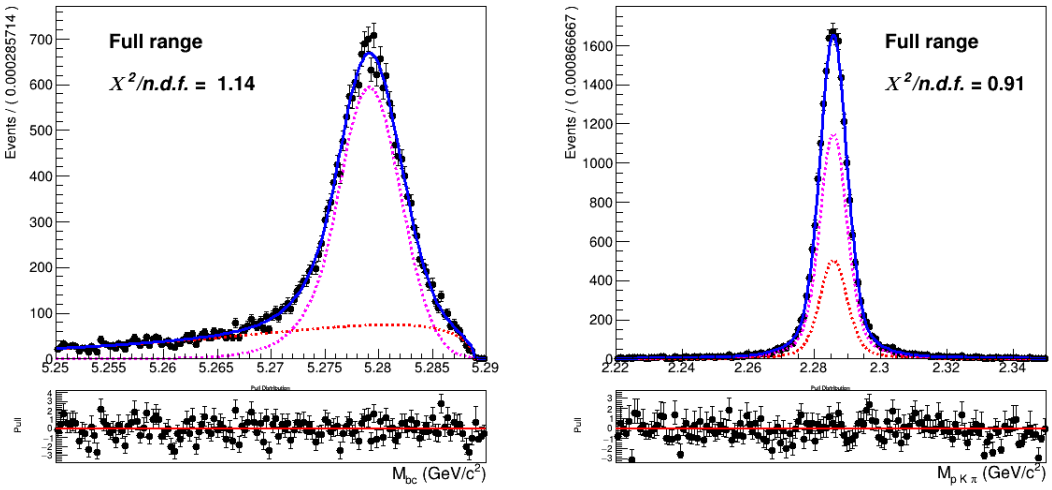

FIG. (12) Two dimensional fit of total signal events in M_{bc} and $M(pK\pi)$

The generic background deriving from other B^+B^- events presents a similar shape of the distribution in M_{bc} (see Fig. 13): the probability density functions used for it are again a Crystal Ball and an Argus. Instead, the flat background in $M(pK\pi)$ can be described with a second order Chebychev polynomial function. The two dimensional PDF in this case is given by:

$$P^{GenBkg}_{B,\Lambda_c}(M_{bc}, M(pK\pi)) = [\Gamma_{CB}(M_{bc}) + \Gamma_{ARG}(M_{bc})] \times \rho_{Cheb2}(M(pK\pi)) \tag{4}$$

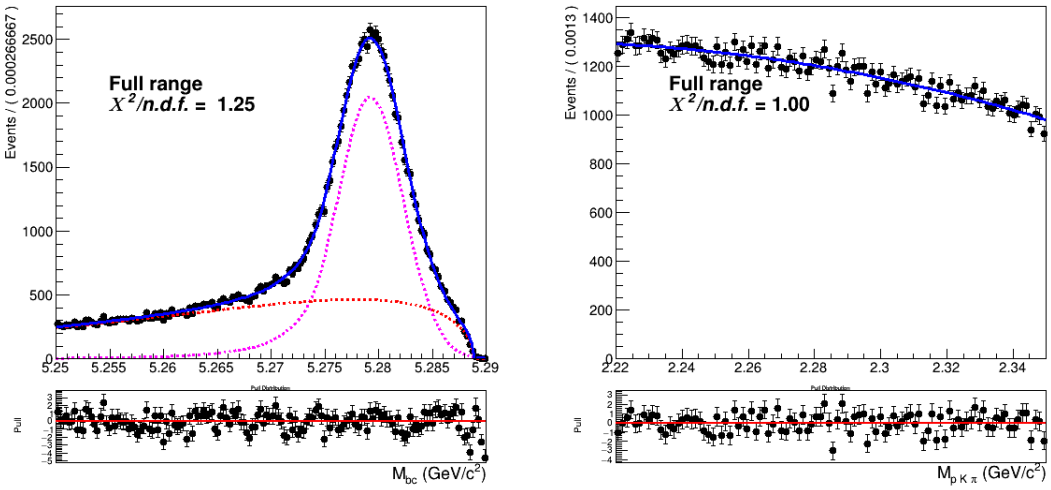

FIG. (13) Two dimensional fit of generic (B^+B^-) events in M_{bc} and $M(pK\pi)$.

The contamination of misreconstructed B^0 events in the B^+ signal (and vice-versa) induces a background which peaks near the B meson mass, as one can see in Fig. 14. Since among the misreconstructed B^0 events there are also $B^0 \to \Lambda_c$ decays (peaking at the Λ_c mass), this background contribution is also named "crossfeed background". The M_{bc} is modelled with a sum of Novosibirsk (colored in magenta) and Argus function (colored in red). Whereas the $M(pK\pi)$ distribution is described by the sum of a first order Chebychev polynomial and the peak by the same sum of three Gaussian functions used to describe the signal peak. In fact the latter is the result of the reconstruction of crossfeed events $B^0 \to \Lambda_c$. Therefore the 2D PDF can be written as:

$$P^{CrossBkg}_{B,\Lambda_c}(M_{bc}, M(pK\pi)) = [\Gamma_{Nov}(M_{bc}) + \Gamma_{ARG}(M_{bc})] \times [\rho_{Cheb1}(M(pK\pi)) + \rho_G(M(pK\pi))] \tag{5}$$

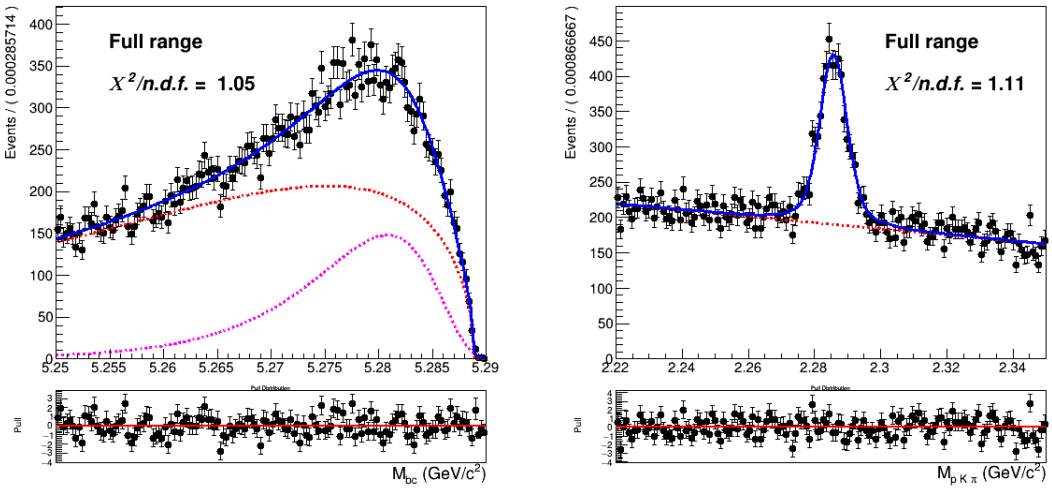

FIG. (14) Two dimensional fit of crossfeed ($B^0\bar{B}^0$) events in M_{bc} and $M(pK\pi)$.

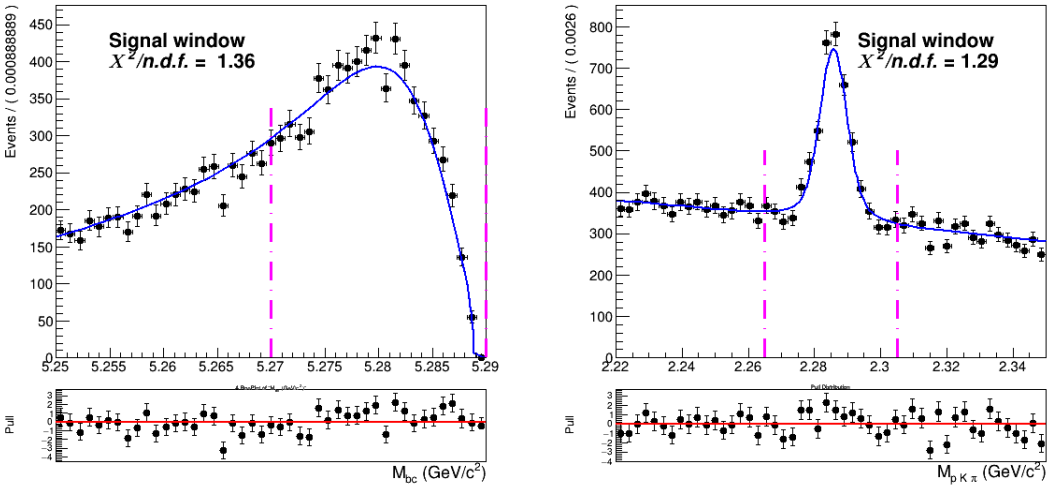

FIG. (15) Signal region projections in M_{bc} and $M(pK\pi)$.

From the projections plotted in Fig. 14 the distributions appear to be well described

by the PDF discussed above. Though the agreement in the Λ_c invariant mass is not fully respected when different regions of M_{bc} are considered, as one can see from Fig. 15 - 16. The fraction of the amount of peaking events is not uniform among different M_{bc} regions. Since this background typology is peaking in both the observables of the fit, the potential correlation between them could have an impact on the signal yield extraction in the total fit.

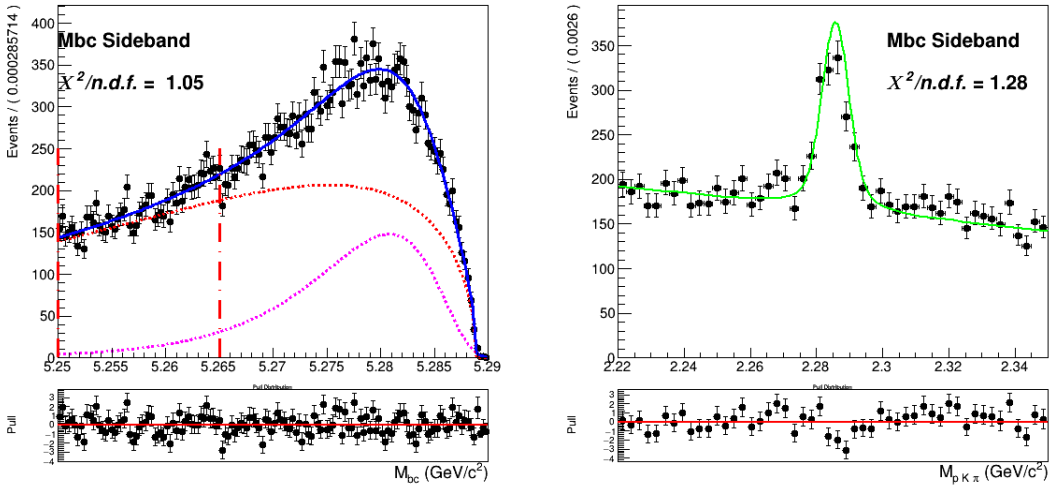

FIG. (16) M_{bc} sideband region projection.

To minimize this effect, and to avoid possible biases deriving from this feature, a correction is attempted. The M_{bc} is divided in 5 different regions. As shown in Figures 17a-17e, for each of these regions a fit on the projected Λ_c invariant mass is performed to extract 5 values of the fraction of peaking events in those regions (all other parameters are fixed). Those values are then used for a parametrization of this parameter as a function of M_{bc}.
From the plot shown in Fig. 18 one can see that it is possible to describe the trend with a linear dependence with a good approximation.

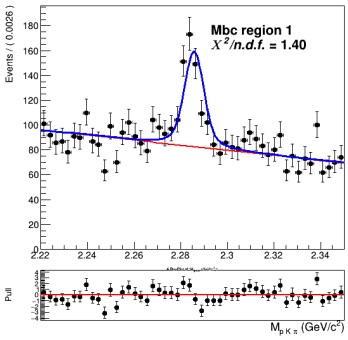

(a) Fit on $M(pK\pi)$ in the region $5.25 < M_{bc} < 5.258$ GeV/c^2.

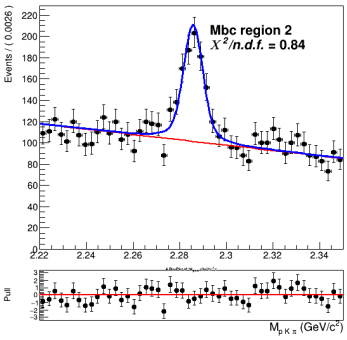

(b) Fit on $M(pK\pi)$ in the region $5.258 < M_{bc} < 5.266$ GeV/c^2.

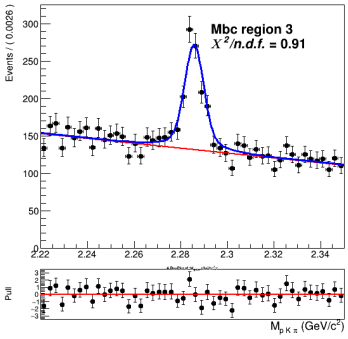

(c) Fit on $M(pK\pi)$ in the region $5.266 < M_{bc} < 5.274$ GeV/c^2.

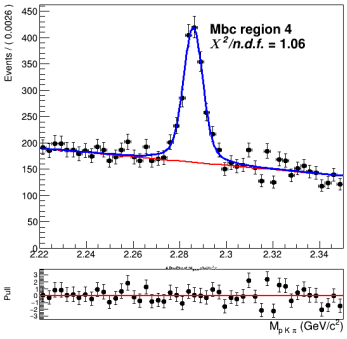

(d) Fit on $M(pK\pi)$ in the region $5.274 < M_{bc} < 5.282$ GeV/c^2.

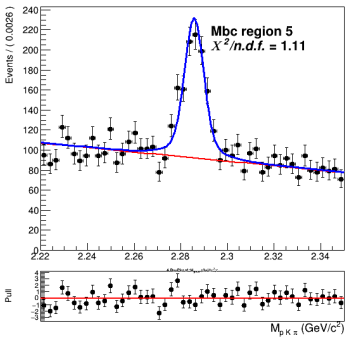

(e) Fit on $M(pK\pi)$ in the region $5.282 < M_{bc} < 5.29$ GeV/c^2.

The 2D PDF describing the crossfeed background is consequently modified:

$$P_{B,\Lambda_c}^{CrossBkg}(M_{bc}, M(pK\pi)) = [\Gamma_{Nov}(M_{bc}) + \Gamma_{ARG}(M_{bc})] \times [F(M(pK\pi)|M_{bc})]$$

where the conditional PDF $F(M(pK\pi)|M_{bc})$ describing the invariant mass is still a sum of $\rho_{Cheb1}(M(pK\pi))$ and $\rho_G(M(pK\pi))$, but their fraction is now parametrized as a function of M_{bc}.
In Figures 19- 20 one can appreciate the improvement obtained with this correction.

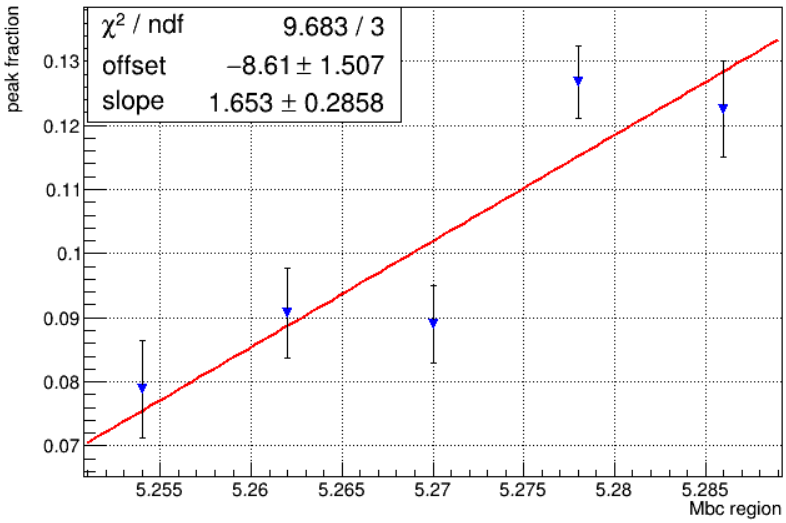

FIG. (18) Invariant mass peak fraction as a function of M_{bc}.

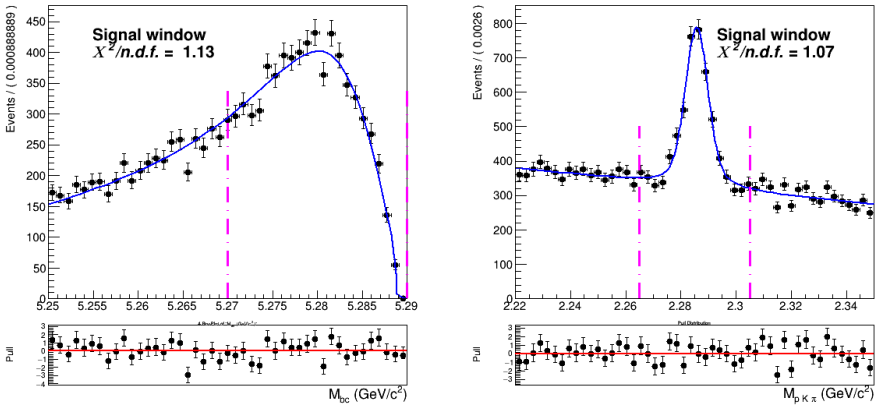

FIG. (19) Signal region projections in M_{bc} and $M(pK\pi)$ after the parametrization.

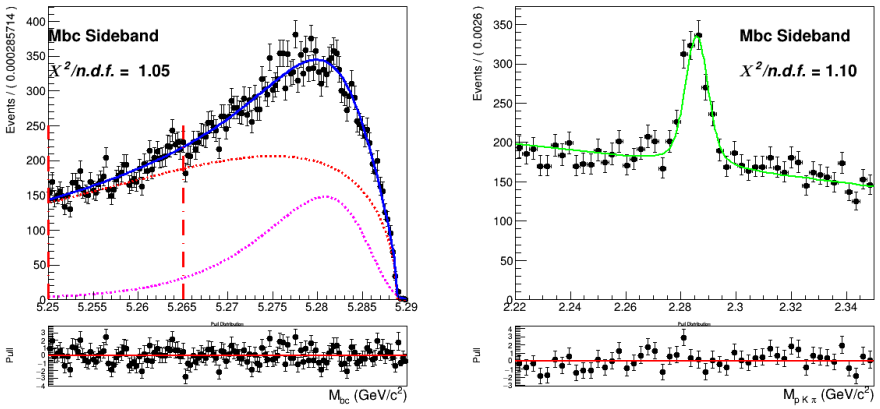

FIG. (20) M_{bc} sideband region projection after the parametrization.

Besides the dataset recorded at the energy of the $\Upsilon(4S)$ resonance ($E_{CMS}^{on-res} = 10.58$ GeV), the *Belle* experiment recorded a sample of 89.4 fb^{-1} at an energy 60 MeV below the nominal $\Upsilon(4S)$ resonance ($E_{CMS}^{off-res} = 10.52$ GeV). The dataset allows to check for an appropriate modeling of the continuum MC simulation.Using the official tables (`https://belle.kek.jp/secured/nbb/nbb.html`) the off-resonance sample is scaled by

$$\frac{\mathcal{L}^{on-res}}{\mathcal{L}^{off-res}} \left(\frac{E_{CMS}^{off-res}}{E_{CMS}^{on-res}} \right)^2 \tag{6}$$

taking into account the difference in luminosity and in E_{CMS} (Energy in center of mass system).

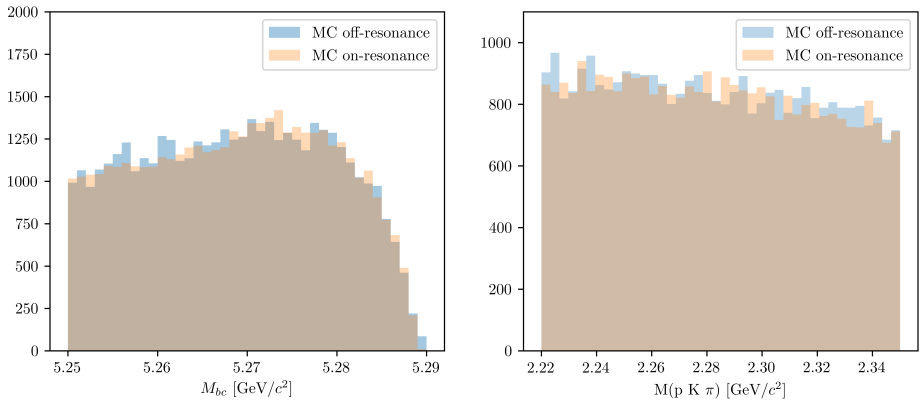

FIG. (21) M_{bc} and $M(pK\pi)$ comparison between on-/off-resonance (scaled) Monte Carlo simulated continuum.

The plot in Fig.21 shows the M_{bc} and $M(pK\pi)$ distributions in the MC on-/off-resonance continuum after the scaling[1].

[1] it is obtained with the MC off-resonance sample being composed of 6 streams: the total amount is normalized

Ideally, provided that there's a good agreement between MC and data for the off-resonance sample and also between the MC on-/off-resonance continuum after the scaling, one could directly use the scaled off-resonance data to describe the continuum background in the fit on data. Since the off-resonance MC (and data) present very low statistics (Fig. 22 shows the Λ_c invariant mass in off-resonance data), scaling them with all the applied selection cuts would cause the PDF describing the continuum to be very much affected by statistical fluctuations. Additionally, since the B meson candidates are reconstructed in both on-resonance and off-resonance events for values of $M_{bc} \geq 5.22$ GeV/c^2, but the E_{CMS} differs, there can be effects of correlations between the applied *SignalProbability* cut and the M_{bc} variable that one needs to take into account. This effects on the M_{bc} are carefully studied in the analysis of the control sample. In Fig. 24 one can notice some discrepancy in the shapes, apart from the not negligible statistical fluctuations in the (scaled) off-resonance distribution. In the Λ_c invariant mass one doesn't expect correlation effects, but nevertheless there can be differences due to the limited statistics of the off-resonance sample. In fact, in the case of on-resonance MC some events in which Λ_c candidates survive nominal selection cuts are visible and can be described with a small Gaussian on the top of the flat background (Fig.27a). On the contrary in the off-resonance sample doesn't show anything beside the flat background (the Fig.27b shows a 5 streams statistics).

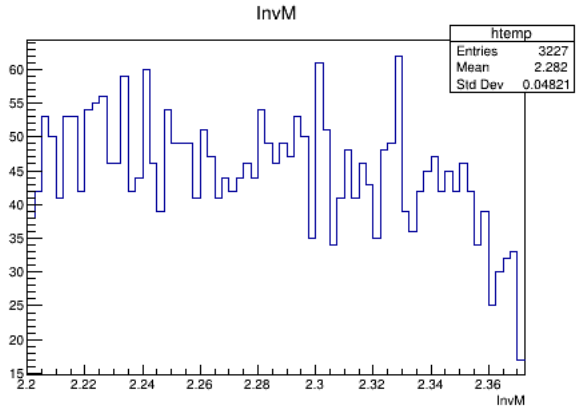

FIG. (22) Λ_c invariant mass in off-resonance data (all cuts applied).

To obtain the shape that can describe the continuum background M_{bc} distribution on data the continuum suppression is not applied on the off-resonance continuum sample, in order to acquire more statistics. Then it has to be scaled (according to Eq. 6 6.1) and corrected for the *SignalProbability* correlated effects. This procedure is validated first on MC samples. This method works if the shape of the M_{bc} distribution doesn't change significantly removing the continuum suppression cut. Figures 23a - 23b show the agreement between the distributions with and without continuum suppression on MC and data respectively.

The scaling and bin-correction procedure was carried out on a sample of 5 streams of on- and off-resonance MC. From a ratio plot, like the one in Fig. 25a, showing the continuum on-resonance distribution in M_{bc} and the scaled continuum on-resonance distribution without the continuum suppression applied, the bin-correction is obtained to correct the off-resonance data in the scaling procedure. The validity of this procedure is first tested on a sixth independent MC sample: Fig. 25b shows the scaled and bin-corrected off-resonance continuum histogram compared with the continuum on-resonance distribution of the independent stream.

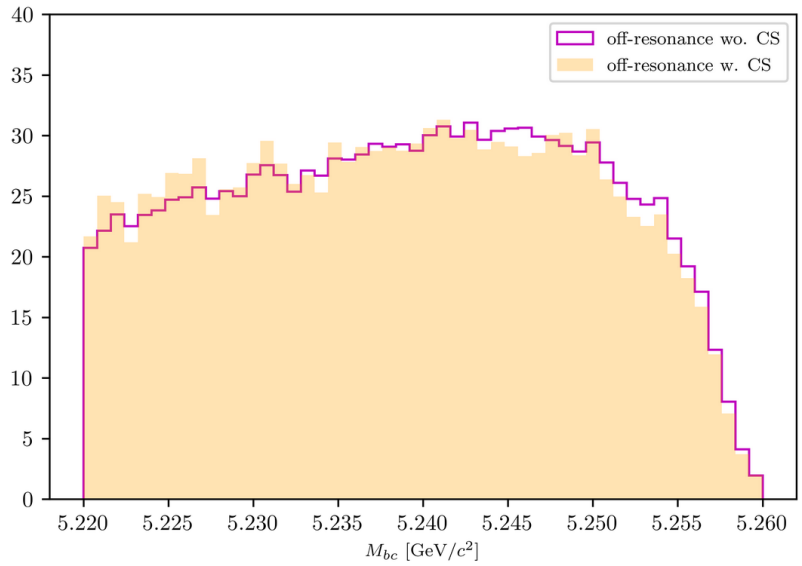

(a)

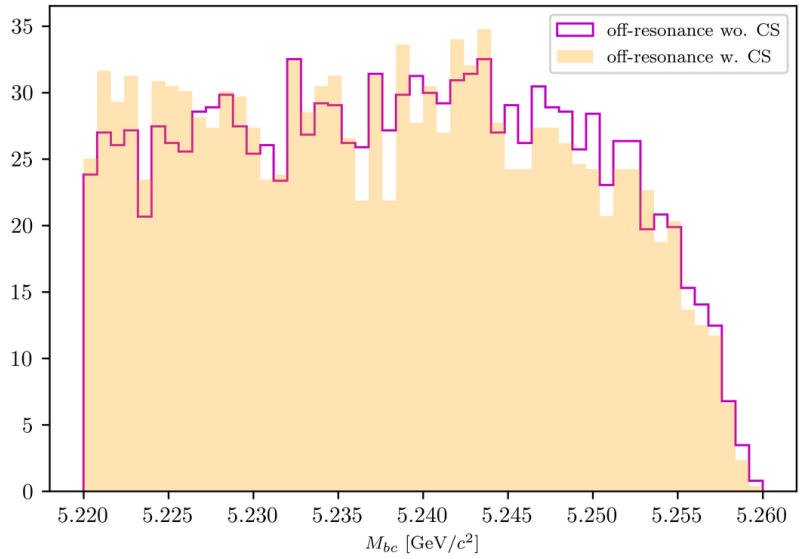

(b)

FIG. (23) Above: M_{bc} distributions of the MC off-resonance sample (5 streams) with and without continuum suppression. Below: M_{bc} distributions on data with and without continuum suppression.

One can see that with this method the scaled simulated off-resonance events agree at reasonable level with the simulated on-resonance continuum. If the on-/off-resonance continuum events are correctly modelled the described method is able to provide a PDF that models continuum events in M_{bc} on data applying it on the off-resonance sample.

The obtained distribution can be then fitted (see Fig. 26), i.e. with a Novosibirsk function.

This is the procedure which can be then applied on the off-resonance data to obtain the M_{bc} shape describing the continuum background in data.

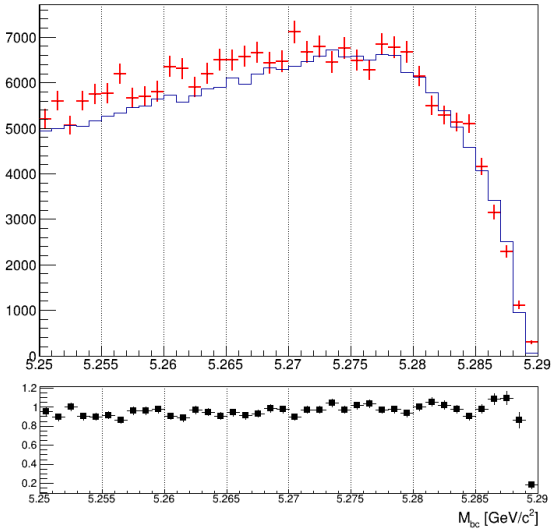

FIG. (24) M_{bc} distributions of the MC (scaled) off-resonance sample (in red) and on-resonance (in blue) using 5 streams statistics and all nominal selection cuts applied.

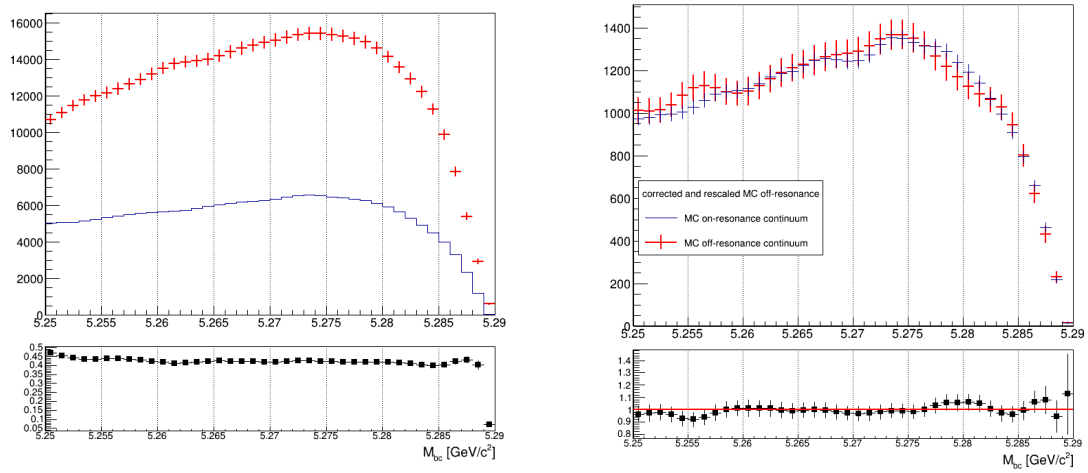

(a) (b)

FIG. (25) On the left: M_{bc} distributions of the MC off-resonance sample without continuum suppression and the MC continuum sample with applied continuum suppression. On the right: M_{bc} distributions of the corrected scaled MC off-resonance and on-resonance MC continuum.

The shape describing the Λ_c invariant mass is obtained from the simulated on-resonance continuum, again using 5 streams statistics (see Fig. 28).

Finally, it is possible to examine the validity of the whole procedure on the independent stream. Fig. 30 shows the M_{bc}, $M(pK\pi)$ projections of the two dimensional fit with the one-dimesional PDFs obtained with the above described procedure. The 2D PDF used can be written as:

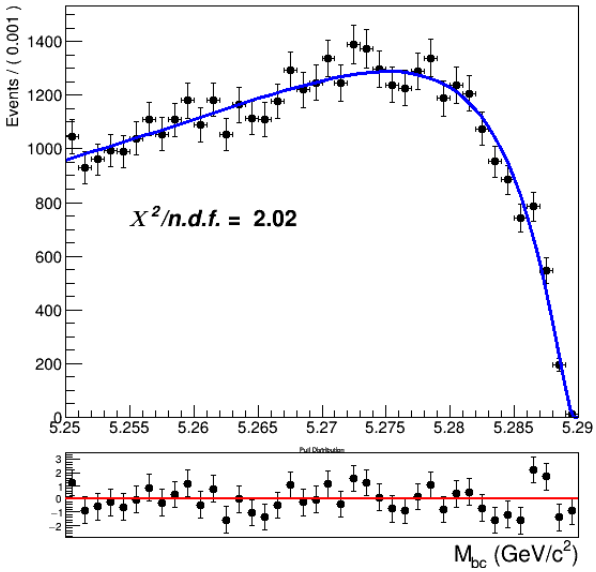

FIG. (26) Fit of the M_{bc} distribution MC (scaled) off-resonance continuum (one stream).

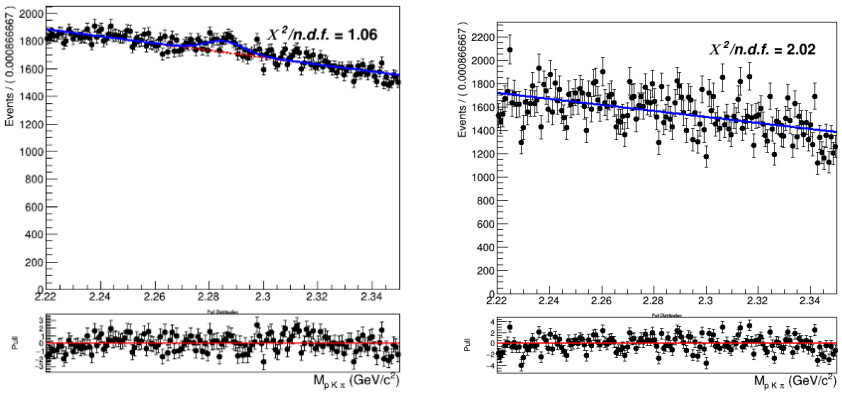

(a) (b)

FIG. (27) Comparison between 5 streams of MC on-resonance continuum 27a) and off-resonance (scaled) continuum in $M(pK\pi)$ (27b).

$$P^{Continuum}_{B,\Lambda_c}(M_{bc}, M(pK\pi)) = \Gamma_{Nov}(M_{bc}) \times [\rho_{Cheb1}(M(pK\pi) + \rho_G 1(M(pK\pi))]$$

where, as already anticipated, the invariant mass is described by a sum of a first order Chebychev polynomial and the peak by a single Gaussian function.

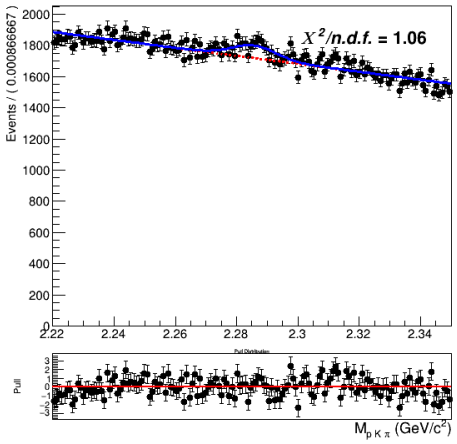

FIG. (28) Fit of the Λ_c invariant mass of on-resonance continuum using the one Gaussian description (all nominal cuts applied).

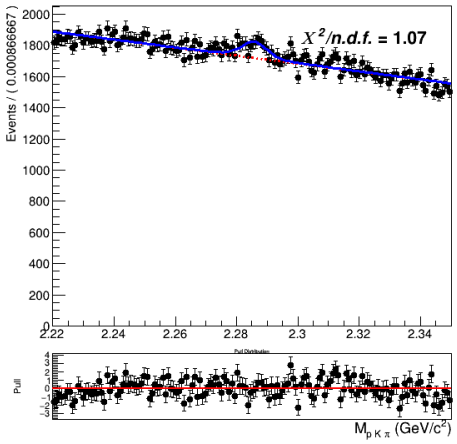

FIG. (29) Fit of the Λ_c invariant mass of on-resonance continuum using the the same three gaussian PDF to describe the peak in the signal invariant mass (all nominal cuts applied).

It was then also investigated to alternatively use the same triple Gaussian PDF to describe the peak, as it is shown in Fig. 29. The two description seem to be equivalent. The final fits described in Sec. 6 6.2 were performed with the one Gaussian description, but it was also tried with the alternative three Gaussian description: no significant difference was noticed and the signal yields differ by only about 10% of the statistical uncertainties. For consistency reasons, on data the second description will be applied.

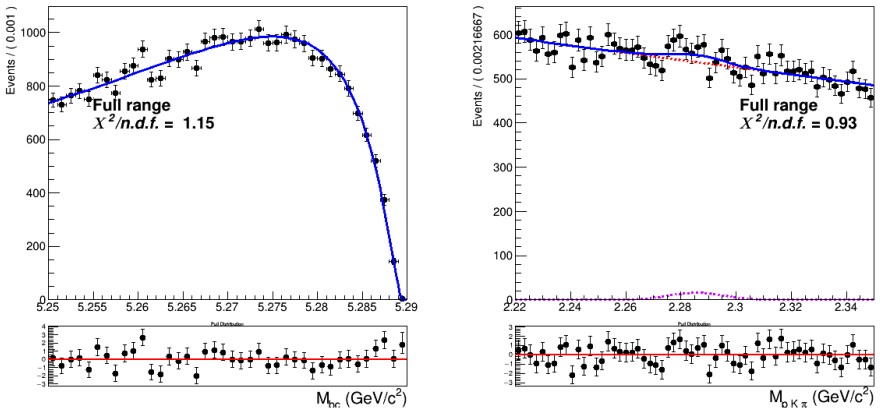

FIG. (30) Two dimensional fit of continuum events (one stream).

6.2. Two dimensional fit

All the already discussed PDFs describing the various categories of events were constructed using five streams. Then an independent stream is used to test if the total PDF enables to extract the signal yield in an unbiased way. In order to test this a total of six fits are performed on six different streams of generic MC. Exemplary, the distributions of stream 0 overlaid by the fitted PDF are depicted in Fig. 31. In all six fits all the shaping parameters are kept fixed, except:

- σ_{G1}: the width of the wider of the three Gaussian functions in $\rho_G(M(pK\pi))$
- σ_{CB} parameter for the Crystal Ball describing the signal

In the M_{bc} distribution the σ_{CB} parameter for the Crystal Ball describing the generic background is expressed as function of the signal σ_{CB} with a ratio fixed from the MC. For the crossfeed background the ratio between its contribution and misreconstructed signal is fixed from the MC.

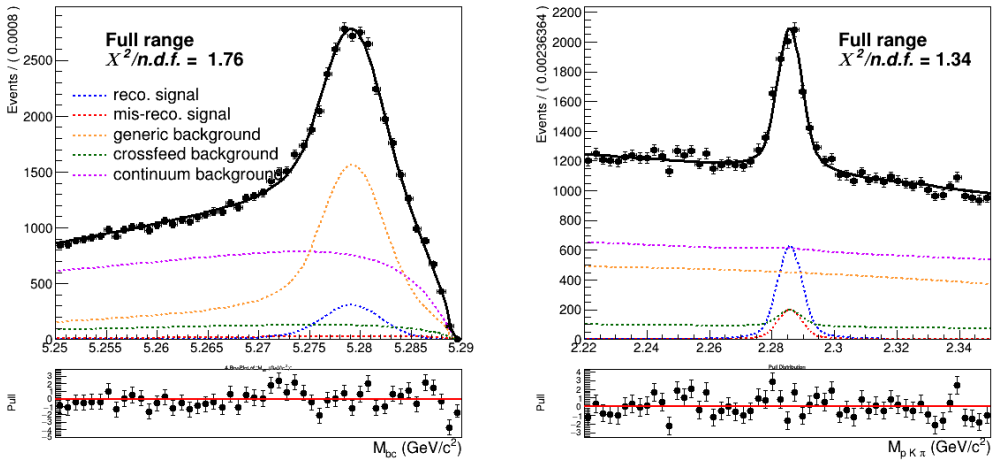

FIG. (31) Two dimensional fit on stream 0 Monte Carlo simulated data.

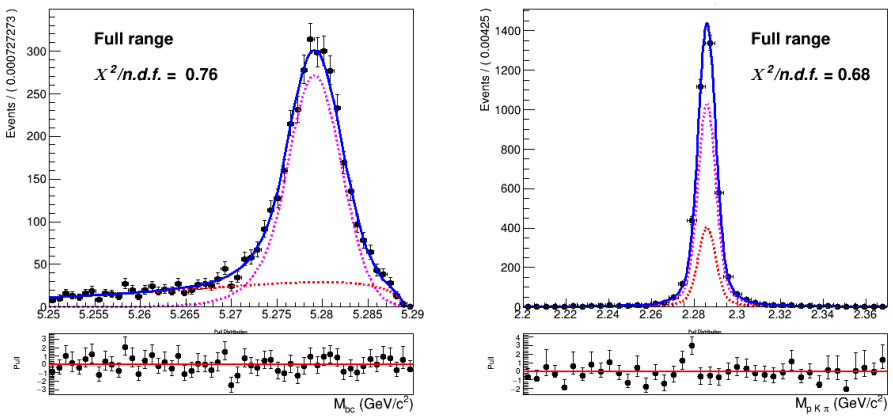

FIG. (32) Two dimensional fit of Total Signal of stream 0 used to extract the expected reconstructed (corresponding to the PDF colored in magenta) and expected misreconstructed yields (corresponding to the PDF colored in red).

The normalizations of mis-/reconstructed signal events and generic background events are floated in the two dimensional unbinned maximum likelihood fits.

In Table I the signal yields of the fits (**Reconstructed Signal**) to the two dimensional distributions for the six streams of $B^- \to \Lambda_c^+$ flavor-correlated decays are listed and compared to the yields obtained from fits of signal distributions of each individual stream. The latter are the "expected" yields of reconstructed signal from a fit to the total signal events in the individual stream as the one plotted on Fig. 32 where all the parameters of the PDFs described by Eq. 6 6.1 - 6 6.1 are kept fixed and the corresponding yields are extracted from the fit.

	Reconstructed Signal		Total Signal			
	fit	expected	fit	MC truth	fit - MC truth	
stream 0	3058± 123	2928 ± 66	4037 ± 121	4061	24	(−0.6 %)
stream 1	3047± 127	2956 ± 66	4098 ± 126	4084	14	(0.3 %)
stream 2	3100± 126	3038 ± 68	4189 ± 125	4267	-78	(−1.8 %)
stream 3	3124± 126	3156 ± 68	4377 ± 125	4337	40	(0.9 %)
stream 4	3125± 128	3048 ± 67	4054 ± 125	4169	-115	(−2.8 %)
stream 5	2909± 127	2816 ± 65	4080 ± 129	4001	79	(2.0 %)
sum	18363	17942	24844	24919	-75	(−0.3 %)

TABLE (I) Comparison of fitted and expected signal yields, fitted and truth-matched total signal for six streams of Belle generic MC when fitting the two dimensional distributions of M_{bc} and $M(pK\pi)$.

Except for stream 3, the fits present slightly higher values of reconstructed signal than expected ones, although always within the 1σ uncertainties (as shown in Fig. 33). The table also reports the fitted and truth-matched number of total signal (sum of reconstructed and misreconstructed signal) events. The values show that deviations are within statistical expectations, which indicates that this sum doesn't present biases. Nevertheless the fact that the reconstructed signal is not fluctuating around zero can be seen as an evidence of a small bias. Fig. 34 shows the differences between fitted and expected values of reconstructed signal with associated uncertainties (calculated as sum of quadrature of both uncertainties

on the results from the fits and the expected values). The performed linear fit shows that, taken together, the six fits present an overall, small but not negligible, bias, which has to be taken into account while fitting the data.

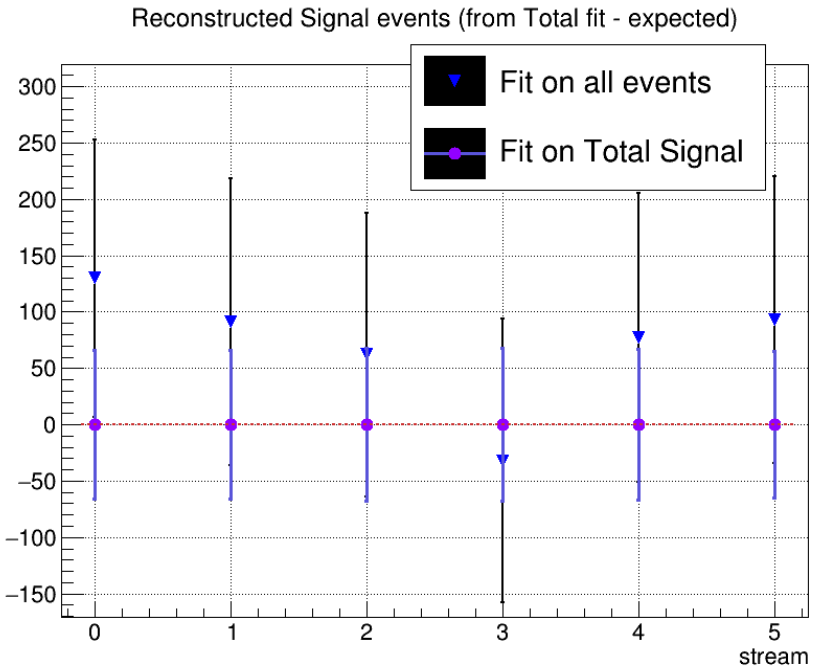

FIG. (33) Differences between results from the fits and "expected" values for signal yields as reported in the first columns on TableI .

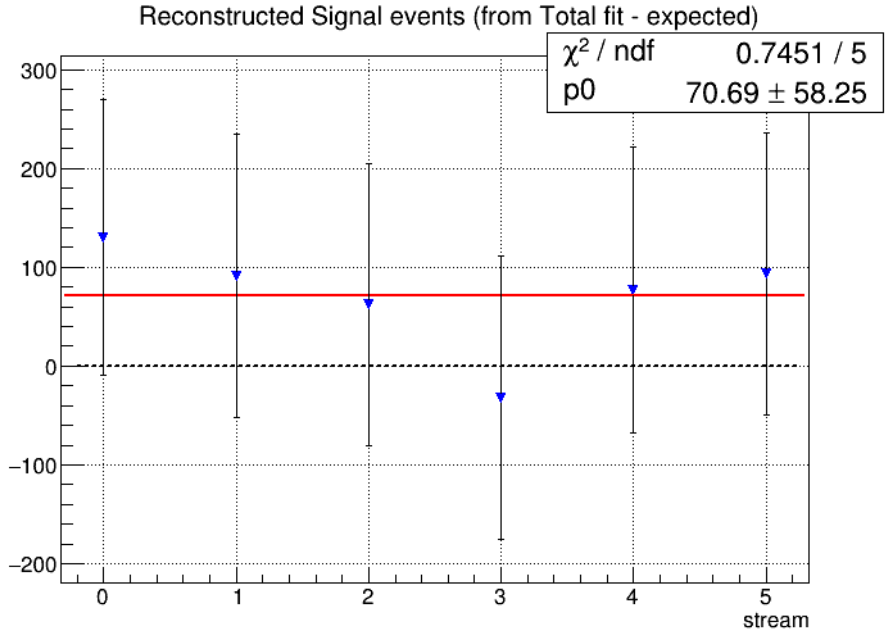

FIG. (34) Fitted-expected subtracted values for reconstructed signal yields with associated uncertainties summed in quadrature.

Additionally, one can investigate the behaviour for different signal-to-background ratio. Thus, a second test of the fit model is performed. Using four independent streams the amount of total signal is varied between 25% and 100% of the nominal values. The amount of background varies according to poissonian fluctuations, as it is taken from four independent streams. The plot in Fig. 35 shows the values of reconstructed signal obtained in the total fits versus those expected by the fits on total signal events. One can see that the values distribute according to a linear dependence. The linear fit suggests a compatibility with a 1:1 relation: the red and the blue dotted lines don't overlap, but the values of the fitted line are compatible within the uncertainties with the identity line. Though also in this second test we see a slight tendency of overshooting the expected values.

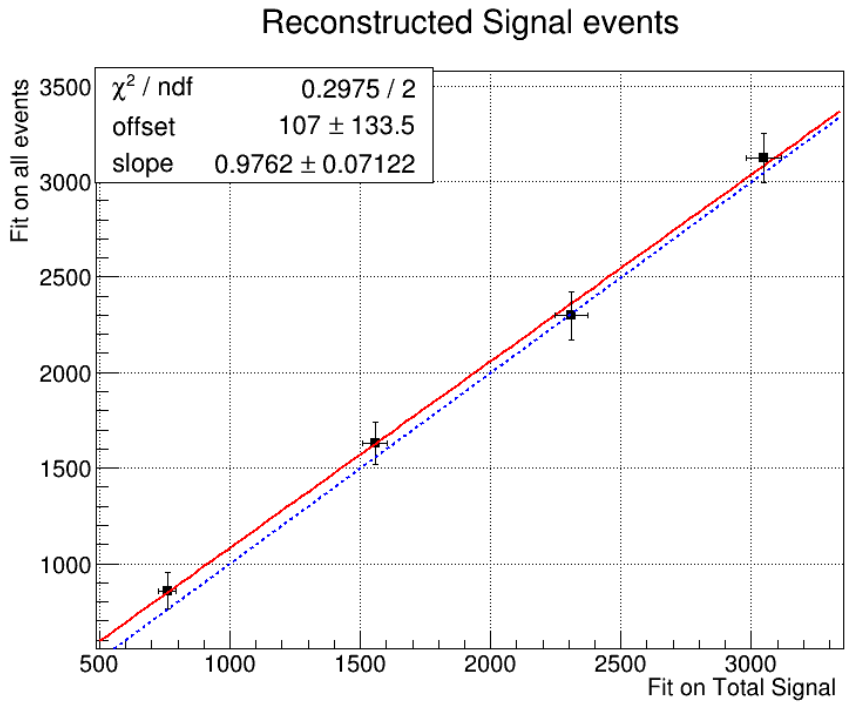

FIG. (35) Linearity test: on the x-axis the obtained reconstructed signal yields from fits on different amounts of total signal; on y-axis the yields of reconstructed signal obtained fitting all events (as in Fig. 31). The values are fitted with a red continuous line, whereas the blue dotted line corresponds to a 1:1 linear dependence.

For the fit model also toy MC pseudo-experiments were performed in order to confirm the behavior of the fit setup. With toy MC experiments the yields, errors and the pulls of the fit are studied by generating our own pseudo-datasets, according to the MC (see Appendix). 3×10^3 pseudo-datasets are constructed, where each dataset was generated with the expected amount of events, distributed according to the Poisson distribution.

6.3. Probability Density Functions (PDFs) for the B_{tag}

The M_{bc} distribution of the tagged B mesons is fitted with a Crystal Ball as for the "peaking" component and the "flat" component is fitted with a Novosibirsk function (Fig. 36). The crossfeed background, consisting of neutral B mesons tagged as charged B, is fitted instead with a sum of a Novosibirsk and an asymmetric Gaussian PDF (Fig. 37).

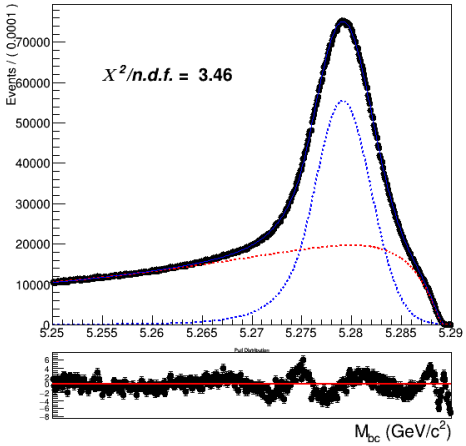

FIG. (36) Fitted distribution of tagged charged B mesons: reconstructed signal events are described by the blue dotted PDF, the misreconstructed with a Novosibirsk function (red dotted).

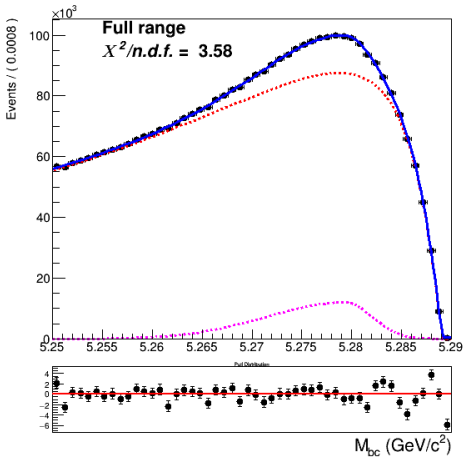

FIG. (37) Crossfeed distribution fitted with a sum of Novosibirsk (red) and asymmetric Gaussian PDF (magenta)

As for the continuum background, a similar procedure as the one described already for the two dimensional fit was adopted:

- first the off-resonance sample is scaled accordingly
- the ratio between the scaled off-resonance and the on-resonance in MC is calculated in each bin (see Fig.38a)

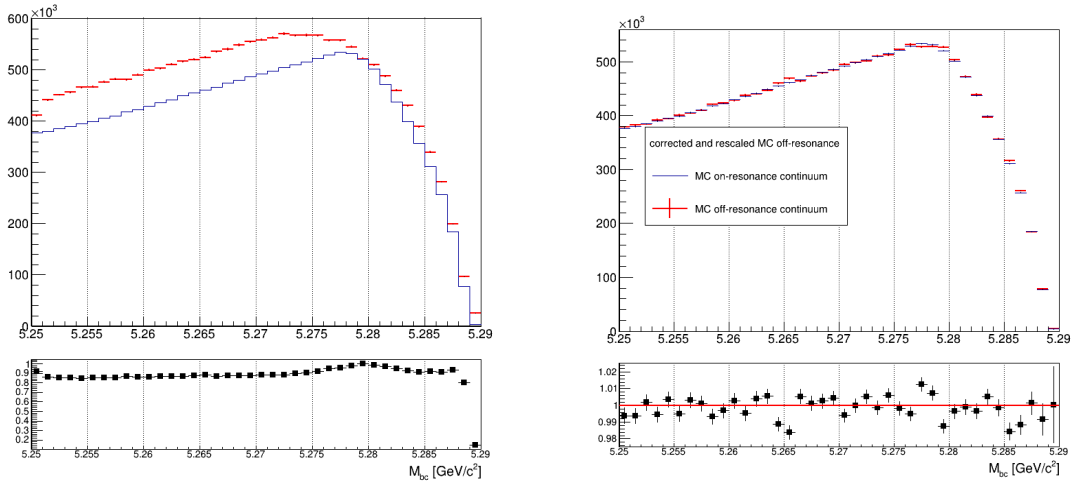

(a) (b)

FIG. (38) On the left: M_{bc} distributions of the MC off-resonance sample and the MC continuum sample with applied continuum suppression. On the right: M_{bc} distributions of the corrected scaled MC off-resonance and on-resonance MC continuum.

- the bin-correction is applied on an independent stream and the scaled and bin-corrected M_{bc} distribution is compared with the on-resonance distribution as shown in Fig.38b

As for the B_{tag} continuum background the statistics is much larger than in the 2D sample, there's no need to remove the continuum suppression cut on the off-resonance sample.

6.4. B_{tag} fit

An independent Monte Carlo stream was used to test the total fit model on tagged B meson candidates. As in the 2D fit, the parameter for the width, σ_{CB}, of the Crystal Ball is floated and the ratio between expected crossfeed background events and misreconstructed signal events is fixed from the MC. The Novosibirsk function describing the misreconstructed signal is also not fully constrained: the parameter describing the tail is free. To avoid introducing significant systematic uncertainties in the fit deriving from the M_{bc} endpoint region, where one has a smearing effect due to variations of the beam energy at the MeV level, the range for the fit is restricted to values betweeen 5.250 and 5.287 GeV/c^2. Yields for the reconstructed and misreconstructed signal are obtained from the fit:

NrecSig	4.2681·10 ^{6}± 5871
NmisSig	5.8787·10 ^{6}± 5128

The Total Signal (the sum NrecSig+NmisSig) is 10146748 ± 4380 (to be compared with 10158571 from the Monte Carlo). This reflects a $\sim 2.5\sigma$ discrepancy between the true MC value and the result from the fit. This can produce some systematic effect, however the normalization does not influence the branching fraction result significantly.

To check the stability of the fit model a toy MC study was performed with 3×10^3 pseudo-datasets (as it was done for the two-dimensional fit model). No evidence for possible biases in the reconstructed signal yields was found (see Appendix).

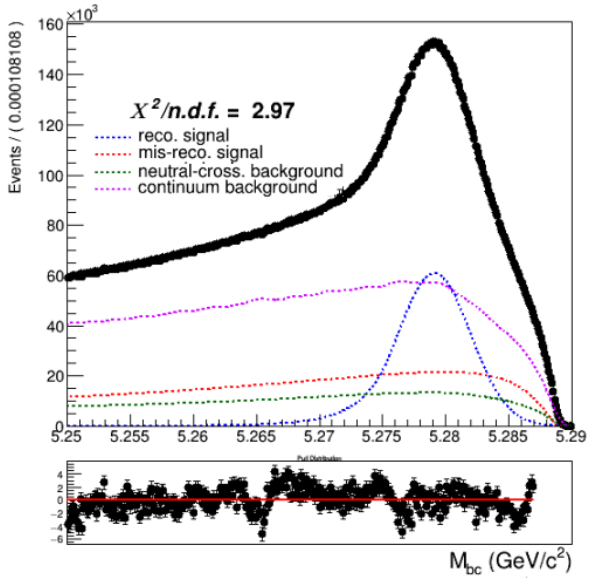

FIG. (39) Total fit of tagged B mesons on Monte Carlo simulated data.

6.5. Λ_c and FEI efficiency

The efficiency in reconstructing the Λ_c baryon after correctly tagging the charged B meson, can be estimated from Monte Carlo simulated data as the fraction of correctly reconstructed signal events that have a correctly reconstructed B_{tag} companion, i.e.:

$$\frac{N_{recSig}(B_{tag}, \Lambda_c)}{N_{recSig}(B_{tag}^{sig})} \tag{7}$$

where $N_{recSig}(B_{tag}, \Lambda_c))$ are the yields of reconstructed signal fro the two dimensional fits (reported in Table I) and $N_{recSig}(B_{tag}^{sig})$ are the yields of correctly reconstructed signal in a fit of B mesons tagged in events where one of the two mesons decayed hadronically and inclusively into a Λ_c baryon (see Fig 40). To minimize statistical uncertainties, in the efficiency calculation the results from all the two dimensional fits were used and six streams of B_{tag} candidates reconstructed in signal events were used for the M_{bc} shown below.

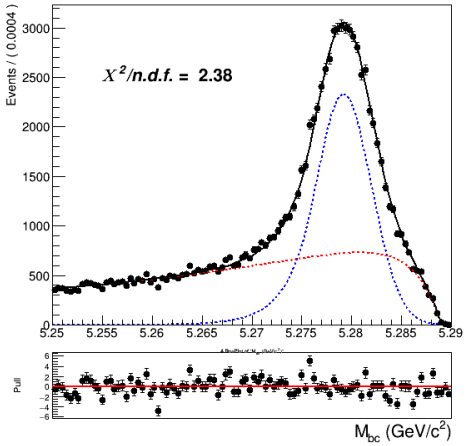

FIG. (40) Fit of tagged B mesons in the "signal events" sample

From this and the results listed in sec. 6 6.2 the efficiency to reconstruct Λ_c is obtained :

$\epsilon_{\Lambda_c} = \frac{NrecSig(B_{tag},\Lambda_c)}{NrecSig(N_{recSig}(B_{tag}} = 44.83 \pm 0.32\%$

The yields from the fit shown in (Fig. 40) can be used also to calculate the FEI tag-side efficiency for signal events, i.e. the efficiency to tag the B meson accompanying a B_{sig} decaying into a Λ_c on the signal side. Whereas results from the fit of charged B_{tag} shown in Fig. 36 can be used to calculate the hadronic tag-side efficiency in the generic B^+B^- events case.

The ratio between the two efficiencies is calculated: $\frac{\epsilon^+_{FEI,sig}}{\epsilon^+_{FEI}} = 0.908 \pm 0.017$

6.6. Studies of Systematic Effects

In Table II the systematic uncertainties of the various considered sources are summarized. Their individual calculation is outlined in the subsequent subsections

source	%
Continuum modeling	0.09
Crossfeed fraction	0.04
$\epsilon^+_{FEI,sig}/\epsilon^+_{FEI}$	0.06
ϵ_{Λ_c}	0.02
Fit bias	0.06
sum	0.27

TABLE (II) Systematic uncertainties in the determination of the $B^+ \to \bar{\Lambda}_c^- X$ branching fractions in %.

6.7. Continuum background modeling

Regarding this source of systematics, one has two take into account two different types. First of all, the continuum background PDFs were obtained based on the limited Monte Carlo statistics. The statistical uncertainties are reflected in the uncertainties on the PDF parameters. Therefore, to estimate this type of uncertainty two-dimensional fits with varied parameters' values by their uncertainties (a fit with +err and −err) were performed. Whereas, the estimation of statistical uncertainty in the case of the B_{tag} should be estimated in principle varying each bin content of its error. On first approximation this is equivalent to vary the nominal number of events described with the histogram PDF by Poissonian variation. Exemplary, fits used to estimate the impact of these uncertainties are shown here in Figures 41 - 42. The yields obtained from those fits for benchmark stream5 results are then compared with the ones already reported previously and a mean deviation value is obtained for both the two-dimensional fit and the B_{tag} fit.

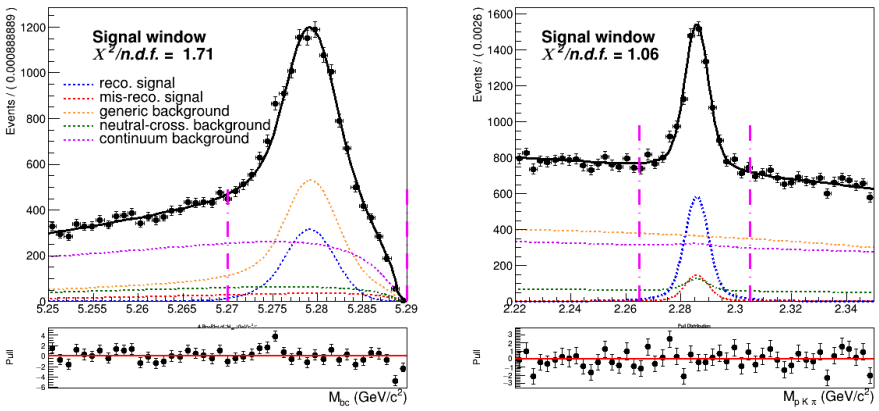

FIG. (41) Signal window projections of a two dimensional fit on Monte Carlo simulated data where the shaping parameters were varied of their uncertainties.

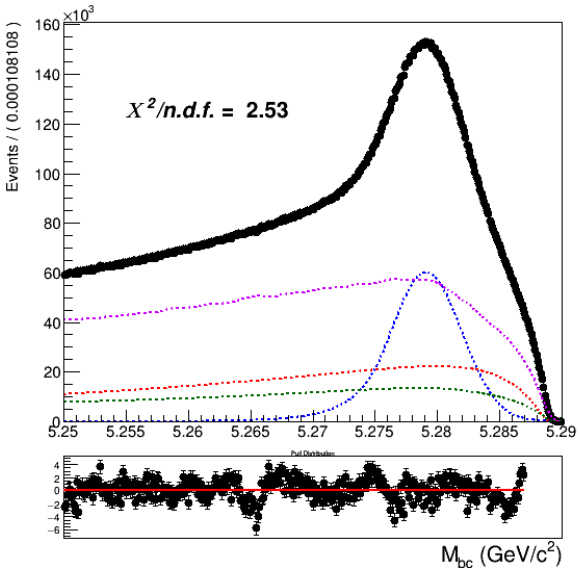

FIG. (42) Fit of tagged B meson candidates on Monte Carlo simulated data where the shaping parameters were varied of their uncertainties.

Fit	$-\sigma$	$+\sigma$	$\pm\bar{\sigma}$
2D	87	- 53	70
B_{tag}	10218	10620	10419

The estimated systematic uncertainty on Br value from this source is 0.07%.

The other type of systematic uncertainty in modeling the continuum is originated by the continuum suppression cut. In fact, when comparing the distribution of the $foxWolframR2$ variable in off-resonance MC and data a slight shift is visible (see Fig. 43). Because of this shift the cut applied on this variable could have a different impact on data, in terms of rejected continuum background. It is found to reject about 60% of the continuum background in data, whereas it rejects 55% of the continuum background in MC (56% in on-resonance MC). The conclusion is that in data one can expect about 2.25% less continuum background events. This discrepancy can be then taken into account when fitting the data sample, applying a simple correction to the number of events. However, the statistical uncertainty on this fraction of events can be also be taken into account as systematics. Being the number of events in the off-resonance data sample without the constinuum suppression applied is very small (less than 10^4), the relative uncertainty on the mentioned fraction of events is negligible compared to the statistical uncertainty on the on-resonance continuum background events in MC: 0.2% compared to 0.6%. Therefore, only the latter source of uncertainty is taken into account and counts for another 0.02% on the BR value.

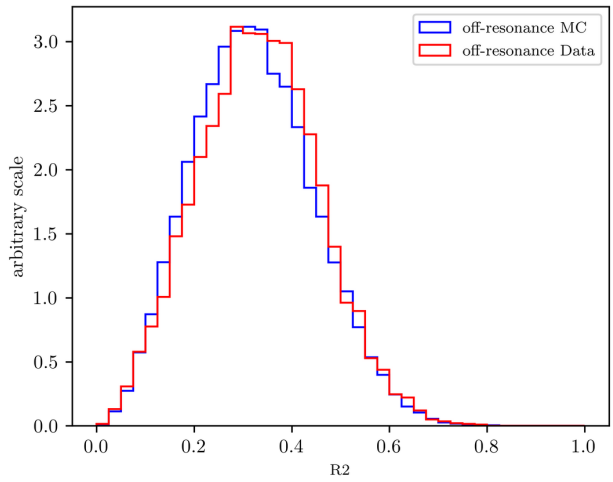

FIG. (43) Distributions of variable $foxWolframR2$ in off-resonance MC and data.

6.8. Crossfeed ratio

The systematic uncertainty on the crossfeed/misreconstructed events' ratio is studied investigating the impact on the yields when considering a plausible discrepancy of this value up to 20% between Monte Carlo and data.

For both the two-dimensional fit and the B_{tag} fit the number of crossfeed events were varied of $\pm 20\%$.

Fit	$-\sigma$	$+\sigma$	$\pm\bar{\sigma}$
2D	24	48	36
B_{tag}	2807	3940	3374

The estimated systematic uncertainty on Br value from this source is 0.04%.

6.9. Efficiencies

The ratio between the two FEI efficiencies is: $\frac{\epsilon^{+}_{FEI,sig}}{\epsilon^{+}_{FEI}} = 0.908 \pm 0.017$
The uncertainity on this value originates a systematic uncertainty of 0.06% on the Br value.

The Λ reconstruction efficiency is determined to be $\epsilon_{\Lambda_c} = 44.83 \pm 0.32\%$. The systematic uncertainty originated by its uncertainty is 0.02% on the Br value.

6.10. Fit biases

The small bias on the reconstructed signal seen in the two-dimensional fit model (see Fig. 34) has to be corrected when fitting data, but the uncertainty on it has to be taken into account in the systematics. Also the discrepancy in the total signal fit result observed in the B_{tag} needs to be included in the systematic effects. Propagating the two sources of systematics in the branching fraction calculation results in an additional 0.06% uncertainty

on the branching fraction value.

6.11. Measured $B^+ \to \bar{\Lambda}_c^- X$ inclusive Branching Fraction

As the measurement is performed considering only the $\Lambda_c \to pK\pi$ decays, to evaluate the inclusive $B^+ \to \bar{\Lambda_c}^- X$ Branching Ratio on Monte Carlo simulated data one needs to take into account the value set for the Λ_c Branching Ratio to the specific decay into that particular final state. The total $Br(\Lambda_c^+ \to pK^-\pi^+)$= 5.53% in Belle Generic MC (including resonant decays). Using the results from the two dimensional fit performed on stream 5 and with all the needed factors known, it's possible to examine the agreement between the expected inclusive $B^+ \to \bar{\Lambda}_c^- X$ Branching Fraction.

Using the expected yields for the two-dimensional fit on stream5 and the B_{tag} fit performed only on signal events, the measured value is $(2.85 \pm 0.07^{stat.})$ %.
Instead from the fit result on stream5 for the two-dimensional fit and the result for the B_{tag} fit shown in Fig. 39, the measured value is $(3.03 \pm 0.13^{stat.} \pm 0.27^{syst.})$ %.

The two measured values using Monte Carlo simulated data agree with each other within statistical uncertainties. Moreover they also show agreement within statistical uncertainties with the value set in the Belle MC (which can be determined by counting method): 2.92%.

Comparing the obtained values with the branching fraction measured by BaBar experiment (see [1]), the uncertainties appear reduced by almost a factor two (statistical uncertainties almost by factor four).

7. APPENDIX

8.

[1] The BABAR Collaboration, B. Aubert, et al, *Study of Inclusive B^- and $\bar{B}^0$ Decays to Flavor-Tagged D, D_s and Λ_c^+*, Phys.Rev.D75:072002,2007.

[2] I.L. Grach et al., Nucl.Phys. B502, 227 (1997)

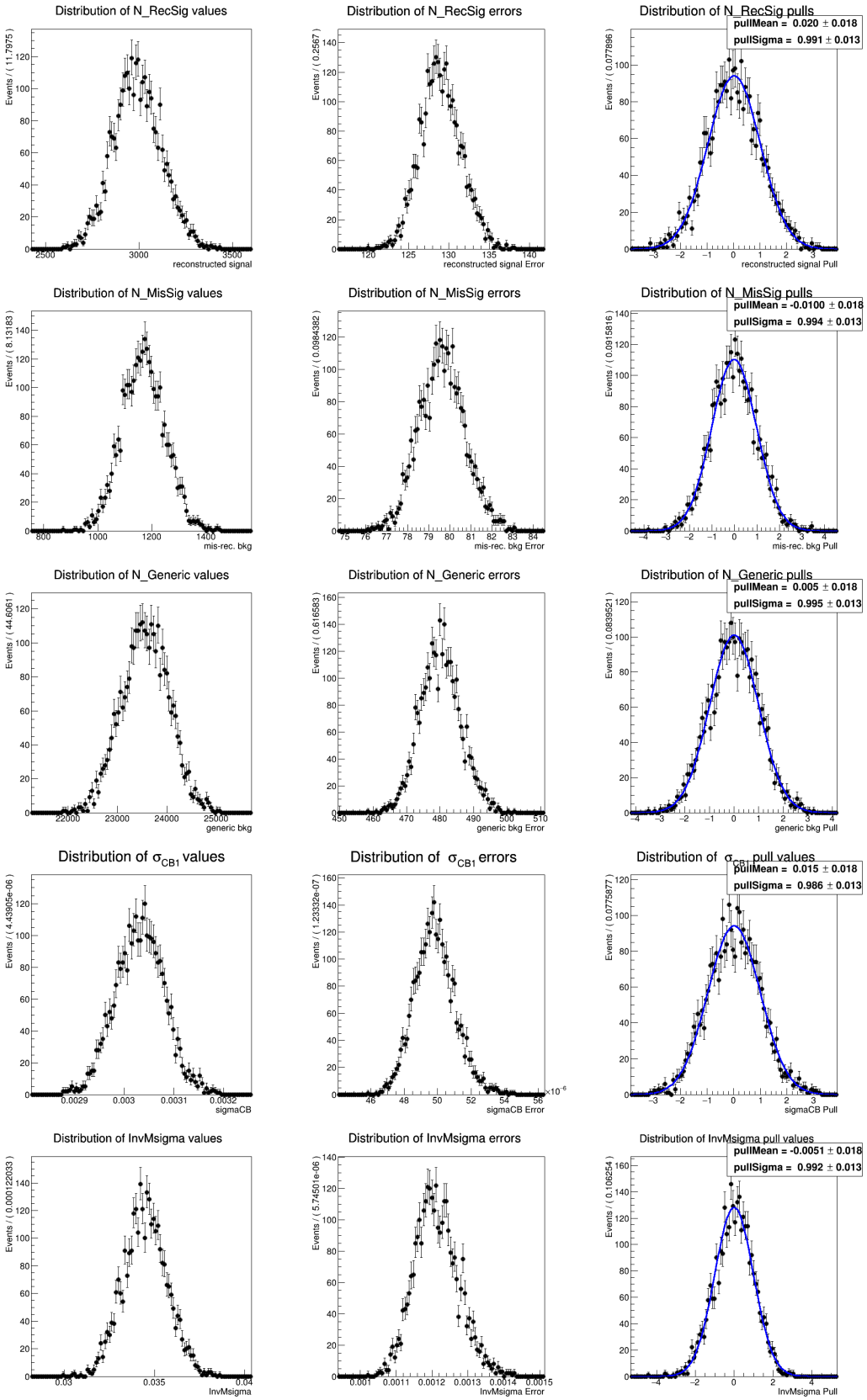

FIG. (44) Toy MC study for the two dimensional fit model described in Sec. 6 6.2

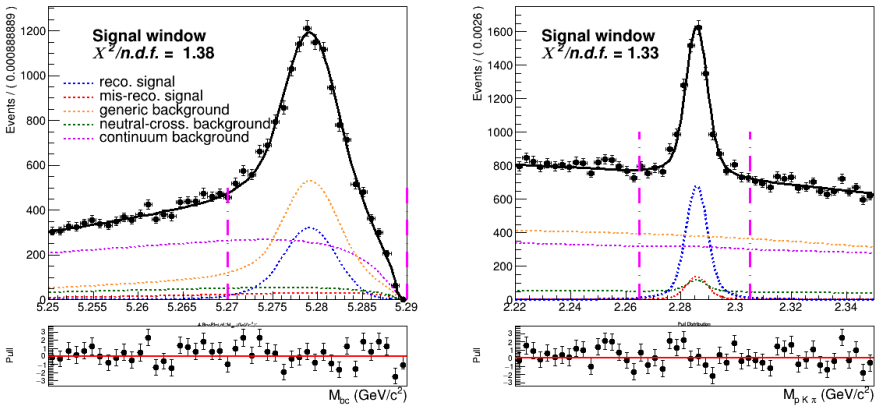

FIG. (45) Signal region ($2.22 < M(pK\pi) < 2.35$ GeV/c^2 and $5.27 < M_{bc} < 5.29$ GeV/c^2) projections pf the dimensional fit on stream 0 Monte Carlo simulated data.

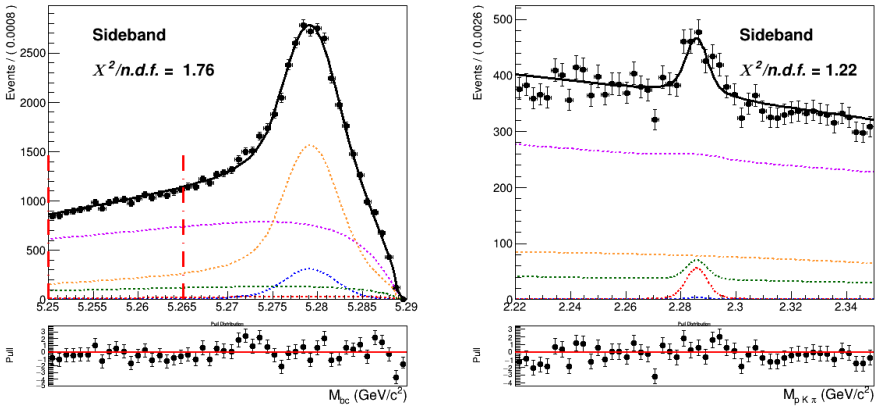

FIG. (46) Sideband region of $5.25 < M_{bc} < 5.265$ GeV/c^2 projection of the two dimensional fit on stream 0 Monte Carlo simulated data.

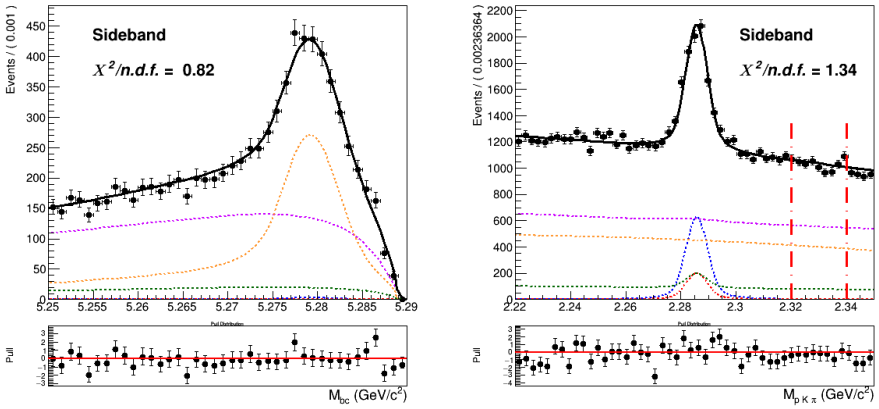

FIG. (47) Sideband region of $2.22 < M(pK\pi) < 2.35$ GeV/c^2 projection of the two dimensional fit on stream 0 Monte Carlo simulated data.

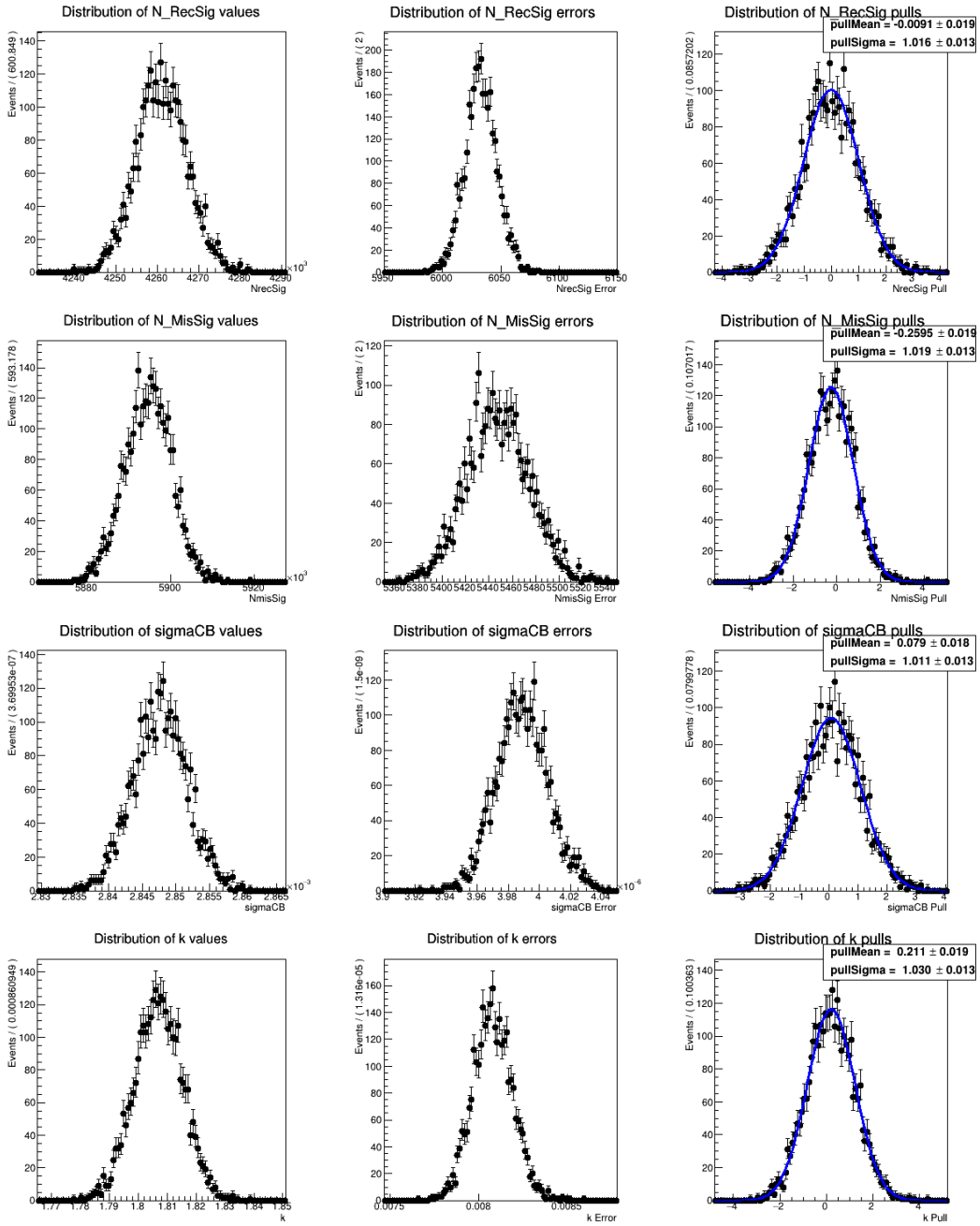

FIG. (48) Toy MC study for the two dimensional fit model described in Sec. 6 6.4